RESEARCH ARTICLE

Simulation of land use trends and assessment of scale effects on ecosystem service values in the Huaihe River basin, China

Xuyang Zhang[1] · Yuzhi Zhou[1] · Linli Long[1] · Pian Hu[1] · Meiqin Huang[1] · Wen Xie[1] · Yongchun Chen[3] · Xiaoyang Chen[1,2]

Abstract

Land use demand change in the Huaihe River basin (HRB) and ecosystem service values (ESVs) in watersheds are important for the sustainable development and use of land resources. This paper takes the HRB as the research object, and using remote sensing images of land use as the data source adopts the comprehensive evaluation analysis method of ESVs based on equivalent factors and sensitivity analysis of the performance characteristics of ESV changes of different land use types. The PLUS model is used to predict spatiotemporal land use change characteristics to 2030 combining inertial development, ecological development, and cultivated land development. The spatial distribution and aggregation of ESVs at each scale were also explored by analyzing ESVs at municipal, county, and grid scales. Considering also hotspots, the contribution of land use conversion to ESVs was quantified. The results showed that (1) from 2000 to 2020, cultivated land decreased sharply to 28,344.6875 km^2, while construction land increased sharply to 26,914.563 km^2, and the change of other land types was small. (2) The ESVs in the HRB were $222,019 \times 10^{12}$ CNY in 2000, $235,015 \times 10^{12}$ CNY in 2005, $234,419 \times 10^{12}$ CNY in 2010, $229,885 \times 10^{12}$ CNY in 2015, and $224,759 \times 10^{12}$ CNY in 2020, with an overall fluctuation, first increasing and then decreasing. (3) The ESVs were $219,977 \times 10^{12}$ CNY, $218,098 \times 10^{12}$ CNY, $219,757 \times 10^{12}$ CNY, and $213,985 \times 10^{12}$ CNY under the four simulation scenarios of inertial development, ecological development, cultivated land development, and urban development, respectively. At different scales, the high-value areas decreased, and the low-value areas increased. (4) The hot and cold spots of ESV values were relatively clustered, with the former mainly clustered in the southeast region and the latter mainly clustered in the northwest region. The sensitivity of ecological value was lower than 1, while the ESV was inelastic to the ecological coefficient, and the results were plausible. The mutual conversion of cultivated land to water contributed the most to ESVs. Based on the multi-scenario simulation of land use in the HRB by the PLUS model, we identified the spatial distribution characteristics of ESVs at different scales, which can provide a scientific basis and multiple perspectives for the optimization of land use structure and socio-economic development decisions.

Keywords Huaihe River basin · Spatiotemporal evolution · Ecosystem service value · Multi-scenario prediction · Multi-scale effects · PLUS model

Introduction

Ecosystem services (ESs) are those life-support goods and services received directly or indirectly through the structure, processes, and functions of ecosystems and whose formation, supply, and distribution are profoundly influenced by land use (Xie et al. 2015). Land creates a large amount of ecosystem service value (ESVs) for humans, and the majority of social and economic activities use it as a carrier. Moreover, land plays a fundamental role in food security and ecological safety, holding a supply value (provision of food, raw materials, and water resources), regulating value (purification of the landscape, gases, climate, and hydrology), supporting value (soils, nutrient cycling, and biodiversity), and cultural value (aesthetic landscape; Costanza et al. 1997).

✉ Xiaoyang Chen
  chenxy@aust.edu.cn

Extended author information available on the last page of the article

With population growth and rapid urbanization (Fan et al. 2022), land use patterns are gradually transforming toward semi-natural and semi-artificial ecosystems (Cumming et al. 2014; Li et al. 2016), and the resulting changes in material and energy flows affect the ability of ecosystems to provide services. Therefore, unsuitable land use will endanger regional ecological security and even limit urban sustainable development (Huang et al. 2021). With the construction of large-scale, long time series and the diffusion of high-intensity human activities, watersheds provide an important material base and ecological services for human survival (Xie et al. 2022). At the same time, as the population gathers in river basins and the scale of a city expands, the demand for ESs such as food supply, water supply, air purification, water containment, and cultural recreation will continue to increase. The HRB (Huaihe River basin) is located in the north–south climate transition zone of China. It is an important ecological barrier, as well as a significant coal and energy base in eastern China, and is a representative case of China for the purposes of this study. The ecological environment and socio-economic development of this region are particularly sensitive to land use changes; hence, it is important to study the land use changes in this basin. In this context, the study of land use impacts on ESV changes in watersheds under multiple scenarios is conducive to the construction of a new pattern of spatial development and protection of watersheds and provides technical support and scientific information.

Changes in land use/land cover directly affect ESVs (Gashaw et al. 2018). Therefore, the estimation of ESVs based on land use changes is the most direct and effective method to quantify the loss of EVS over time. The spatial pattern of ESVs reflects the spatial and temporal evolution of regional ecosystems, which is important to identify regional ecosystem service problems, maintain balanced regional ecological development, and promote regional sustainable development. ESV is a quantitative estimate of the capacity of ESs and can be assessed in two main ways: monetization and energetic valuation (Li 2019). The monetary form of ESV can be easily understood by people and used by decision-makers; it can effectively assist spatial planning, ecological control, and ecological restoration and is widely used (Crossman and Bryan 2009; Crossman et al. 2011; Groot et al. 2012). ESVs are the basis to describe the spatiotemporal evolution of ESs; hence, their accurate accounting is critical. At present, several scholars in China and abroad have generated a wealth of research results on the effects of land use change on ESVs (Assefa et al. 2021; Hu et al.

2022; Song et al. 2017; Tan et al. 2020). In 1997, Constanza et al. developed ESV coefficients for different land use types based on an assessment of global ESVs, which laid the foundation for related studies. Xie et al. (2008) established a base equivalence scale for ESVs in different regions of China, which has been used by a wide range of scholars. ESVs have been explored in relation to three main topics: definition and classification (Braat 2012), value assessment (Xie et al. 2017), and the relationship between ecosystems and social development (Garcia et al. 2018). Specifically, several studies focused on the underlying theory, driving mechanisms, and spatiotemporal variability of ESs, covering national, regional, provincial, municipal, and county scales. In this study, we considered the special situations of different years and regions, continuously improved the adjustment of value coefficients, conducted an assessment of the spatiotemporal variation patterns of regional ESV under different scales of land use changes, and proposed optimized temporal sequencing schemes and spatial development strategies and differences in ESV under different scenario simulations.

Land use patterns can affect ESVs. With the advancement of research, scholars have tried to analyze future land use changes and their impacts on regional ESVs to develop sustainable land use measures Land use simulation is a current research hotspot, and related studies have been conducted using CLUE-S (Niu et al. 2021), SLEUTH (Niu et al. 2021), SD (Bing et al. 2016), FLUS (Liu et al. 2021), and CA-Markov (Guzman et al. 2020), among others. The Patch-generating land use simulation (PLUS; Liang et al. 2021), as a new land use simulation model, has higher simulation accuracy than the commonly used prediction models, and its results can better support policies and sustainable development. Xie et al. (2022) found that ESVs were assessed based on general scenarios and single scales, and comparisons of ecological conservation, cultivated land conservation, and multi-scenario ESVs have been relatively weak. Previous studies focused on a single scale based on macro- (Ye et al. 2021) or micro-scale grid cells (Gao et al. 2021), thereby lacking multi-scale coupled exploration. For example, Liu et al. (2019) assessed the impact of urbanization-induced land use change on ESs under a general scenario and developed an ESV matrix of land use shifts; while Arowolo et al. (2018) assessed ESV changes in response to land use dynamics in Nigeria based on a graphical use shift approach. However, ESVs under a single scenario cannot reveal the differences between natural development and ESVs under the constraints of other policy scenarios, which hinders their

ability to optimize land use structure and measure the trade-offs between socio-economic development and ecological conservation.

Therefore, this paper simulated use changes in the HRB under four scenarios of natural development, ecological development, cultivated land development, and urban development to 2030. Five periods of land use data were used from 2000, 2005, 2010, 2015, and 2020, with the help of the PLUS model. The spatial distribution of ESVs at different scales was explored by combining municipal, county, and grid scales. On this basis, a hotspot analysis was performed to assess the spatial distribution of ESVs under different preferences and the degree of aggregation; moreover, the contribution of land use transformation to ESV change was introduced to explore the influence of land use transformation on ESVs. The results provide a scientific basis for optimizing land use structure and environmental protection in the HRB.

Materials and methods

Overview of the study area

The Huaihe River is one of the seven major rivers in China, originating at the northern foot of Taibai Peak in Tongbai Mountain, Henan Province, and flowing from west to east through the four provinces of Henan, Hubei, Anhui, and Jiangsu, with a total length of about 1000 km. The HRB (30°55′–36°36′N, 111°55′–121°25′E) spans 47 prefectures in the five provinces of Henan, Anhui, Hubei, Jiangsu, and Shandong. It has an area of 480,000 km^2, with an average annual temperature of 11–16 °C and an average annual precipitation of about 927 mm. With a dense population, fertile land, abundant resources, and convenient transportation, it is an important base for grain production, energy and mineral extraction, and manufacturing in China (Fig. 1).
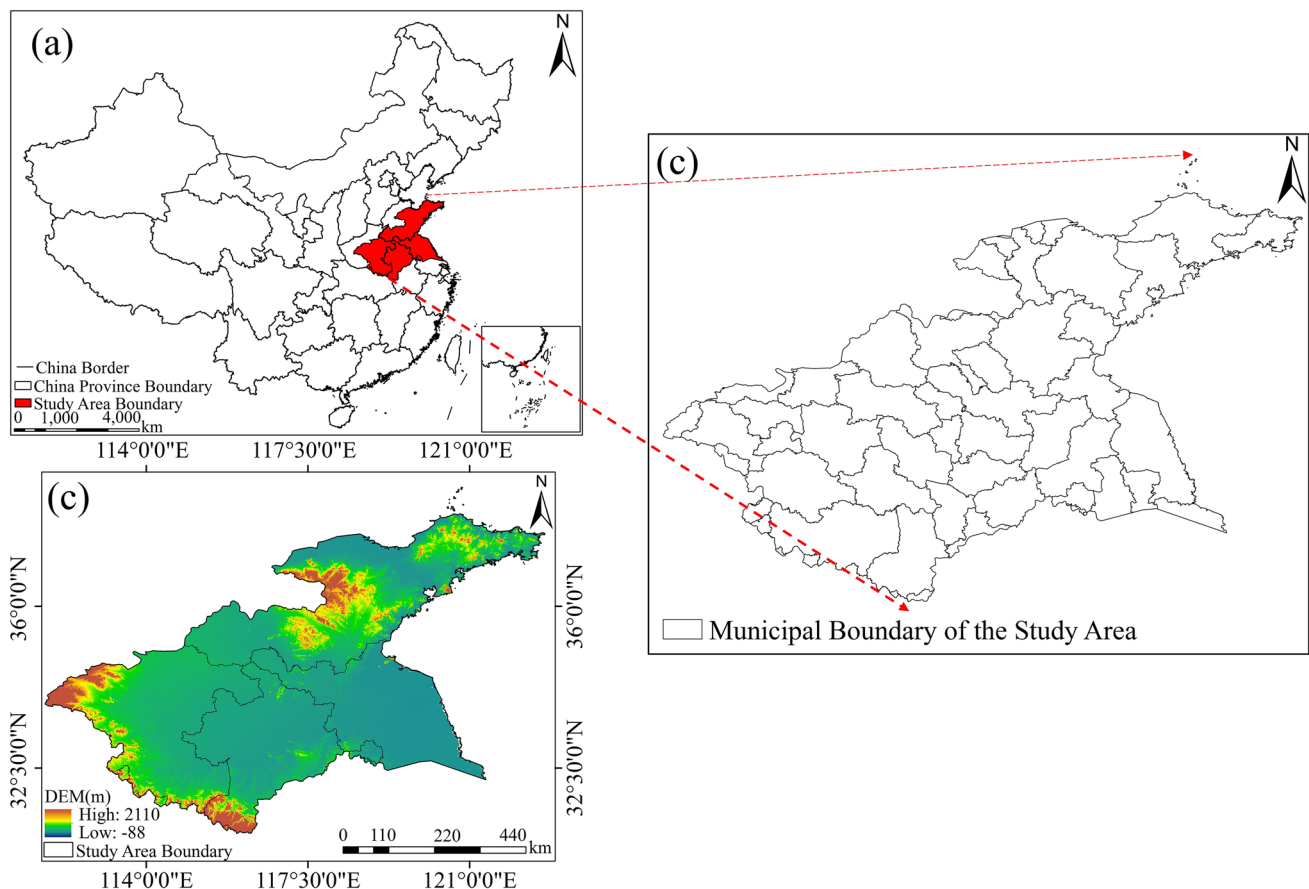

Fig. 1 Geographical location of the study area: (**a**) location of the HRB in China; (**b**) location of administrative cities within the HRB; (**c**) elevation distribution of the HRB

Table 1 Description of driver factor data

Data type	Data name	Data source
Land use data	Land use in 2000	http://data.ess.tsinghua.edu.cn/
	Land use in 2010	
	Land use in 2020	
Land use conversion-limiting factors	Open water	http://data.ess.tsinghua.edu.cn/
	Nature Reserves	http://www.geodata.cn/data/
	Impervious surface	https://data.casearth.cn/
	Cultivated land	http://data.ess.tsinghua.edu.cn/
Driving factors	DEM	https://www.resdc.cn/
	Slope	by DEM data
	Aspect	by DEM data
	Temperatures	https://www.resdc.cn/
	Precipitation	https://www.resdc.cn/
	Potential evapotranspiration	https://www.resdc.cn/
	Population density	https://www.worldpop.org/
	GDP	https://www.resdc.cn/
	Nighttime lighting data	https://www.ngdc.noaa.gov/eog/viirs/download_dnb_composites.html
	Distance from road	https://master.apis.dev.openstreetmap.org/#map=4/36.96/104.17
	Distance from railroads	https://master.apis.dev.openstreetmap.org/#map=4/36.96/104.17
	Distance from rivers	https://master.apis.dev.openstreetmap.org/#map=4/36.96/104.17
	Distance from stations	https://master.apis.dev.openstreetmap.org/#map=4/36.96/104.17
	Distance from buildings	https://master.apis.dev.openstreetmap.org/#map=4/36.96/104.17
	Distance from settlements	http://gaohr.win/site/blogs/china-villages.html
	Soil types	https://www.resdc.cn/
	Soil erosion types	https://www.resdc.cn/
	Vegetation types	https://www.resdc.cn/

Data sources

Total crop coverage, production, and yields for 2000, 2005, 2010, 2015, and 2020 were obtained from the statistical yearbooks of each municipality in the study area and the National Compilation of Agricultural Product Cost Craft Resources for 2000–2020. Data such as constraints used to describe land use conversion (Table 1) were employed to determine meta-cellular conversion rules.

Research framework

In this study, we analyzed the spatial and temporal evolution of land use in the HRB from 2000 to 2020. We simulated scenarios for inertia, ecological land, cultivated land, and urban development in 2030 based on the PLUS model combining five-dimensional drivers. We quantified the ESVs and ESVs granularity of land use at municipal, county, and grid scales. Then, we explored the spatial distribution of ESVs at multiple scales based on hotspot analysis and introduced the degree of contribution of land use conversion to ESVs within a specific framework (Fig. 2).

Research methods

Ecosystem service value (ESV) estimation

In this paper, the equivalence factor method (Table 2) established by Xie et al. (2008) was used to estimate the ESVs in the HRB for five periods from 2000 to 2020, based on the actual land types of the study area. Changes in ESVs were analyzed over multiple years.

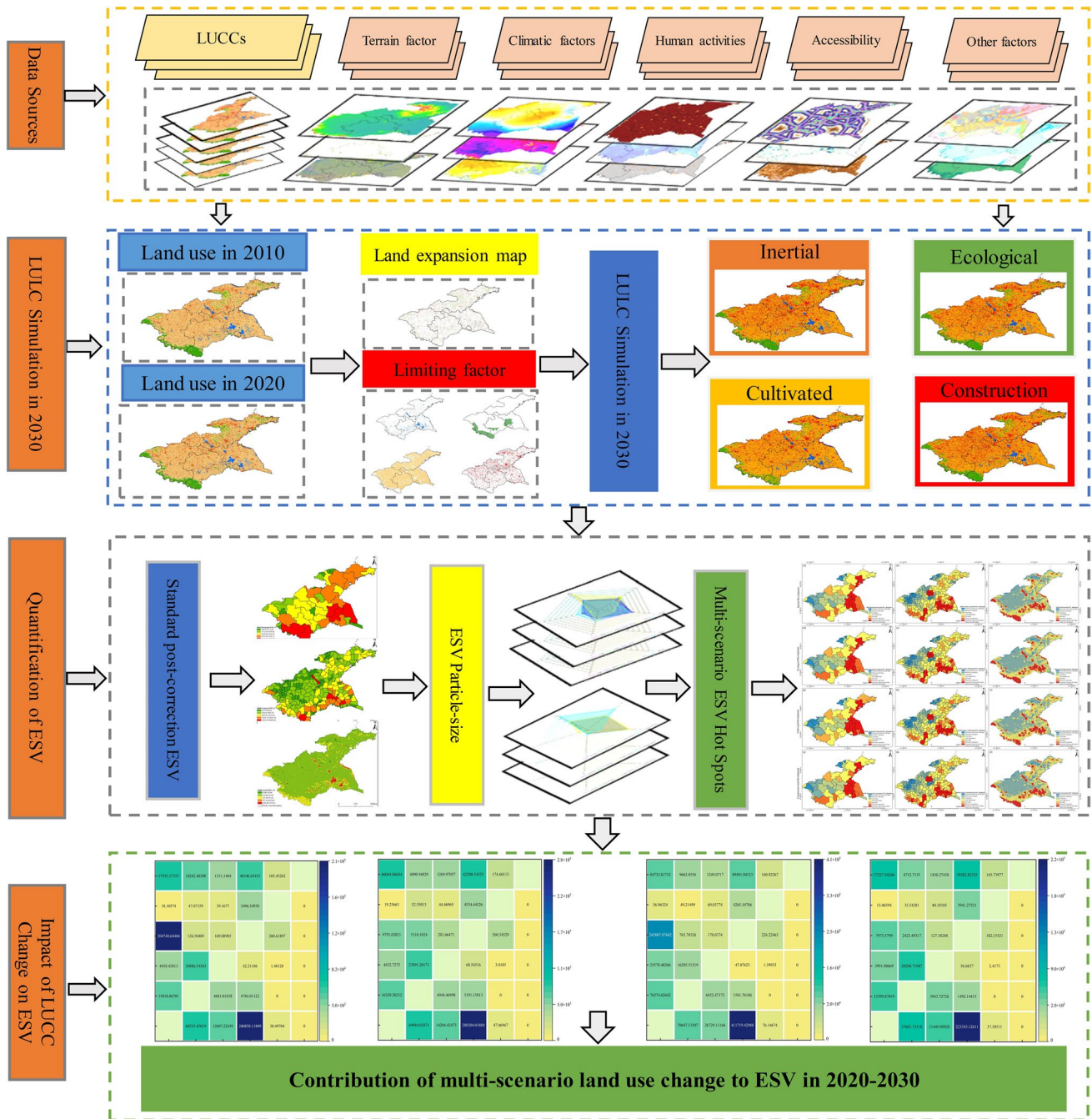(1) Determination of the economic value of one standard unit of ESs

Fig. 2 Research framework

The economic value of natural cereal produced by 1 ha of plowland was considered an equivalent value of the ecosystem. The equivalent value of a standard ES is worth seven times the economic value of grain produced per unit area in that year. Given the availability of statistical data, the economic value of the main food crops (i.e., wheat, corn, and soybean) in the urban areas of the study region from 2000 to 2020 was selected for correction, and their average value was calculated using Eq. (1). The ESV of one standard unit in the study area was 45,010.88613 CNY·hm^{-2}a^{-1}.

$$E_a = \frac{1}{7} \sum_{i=1}^{n} \frac{m_i p_i q_i}{M} \tag{1}$$

Table 2 Ecosystem service value equivalent per unit area

	Ecosystem service type	Cultivated land	Forest	Grassland	Water	Construction land	Unused land
Provisioning	Food production	0.85	0.23	0.23	0.655	0	0.01
	Raw materials	0.4	0.54	0.34	0.365	0	0.03
	Water resource supply	0.02	0.28	0.19	5.44	0	0.02
Regulating	Gas regulation	0.67	1.76	1.21	1.335	0	0.11
	Climate regulation	0.36	5.27	3.19	2.945	0	0.1
	Environmental Purification	0.1	1.57	1.05	4.575	0	0.31
	Hydrological regulation	0.27	3.81	2.34	63.235	0	0.21
Supporting	Soil conservation	1.03	2.14	1.47	1.62	0	0.13
	Maintenance of nutrient cycling	0.12	0.16	0.11	0.125	0	0.01
	Biodiversity	0.13	1.95	1.34	5.21	0	0.12
Culture	Aesthetic landscape	0.06	0.86	0.59	3.31	0	0.05

where E_a is the economic value of one standard ecosystem service unit in CNY·hm^{-2}a^{-1}, i is the type of food crop, m_i is the average price of the i-th food crop in the study area in CNY/kg, P_i is the yield of the i-th food crop in kg/hm^2, q_i is the planted area of the i-th food crop in hm^2, and M is the total planted area of the food crop in hm^2.

(2) Calculation of the ESV

The ESV of the study area was calculated as follows:

$$ESV = \sum_{i=1}^{n} A_i \times VC_i \tag{2}$$

$$VC_i = \sum_{j=1}^{k} EC_j \times E_a \tag{3}$$

where ESV is ecosystem service value in CNY/year, i is the land use type, j is the ecosystem service type, A_i is area of type I land use in hm^2, VC_i is the ESV per unit area of the i-th land use type in CNY and of the i-th food crop in the study area in CNY·hm^{-2}a^{-1}, and EC_j is the j-th ESV equivalent of a given land use type. Because the ESV indicator of construction land was 0 or negative, it was not considered in this paper. K is the number of ecosystem service types; and E_a is the economic value of one standard ecosystem service unit in CNY·hm^{-2}a^{-1}.

(3) Correction based on the biomass factor of the study area

Because of the large area of the HRB, the wide distribution of vegetation cover, and the large differences between the ecosystem and other regions in China, the ESV coefficients needed further revision. In this paper, we referred

Table 3 Ecosystem service value equivalent per unit area in the HRB

	Ecosystem service type	Cultivated land	Forest	Grassland	Water	Construction land	Unused land
Provisioning	Food production	54,328.14	14,700.56	14,700.56	41,864.63	0.00	639.15
	Raw materials	25,566.18	34,514.35	21,731.26	23,329.14	0.00	1917.46
	Water resource supply	1278.31	17,896.33	12,143.94	347,700.09	0.00	1278.31
Regulating	Gas regulation	42,823.36	112,491.21	77,337.70	85,327.14	0.00	7030.70
	Climate regulation	23,009.56	336,834.47	203,890.31	188,231.02	0.00	6391.55
	Purification of the environment	6391.55	100,347.27	67,111.23	292,413.22	0.00	19,813.79
	Hydrological regulation	17,257.17	243,517.90	149,562.17	4,041,694.01	0.00	13,422.25
Supporting	Soil conservation	65,832.92	136,779.08	93,955.72	103,543.04	0.00	8309.01
	Maintenance of nutrient cycling	7669.85	10,226.47	7030.70	7989.43	0.00	639.15
	Biodiversity	8309.01	124,635.14	85,646.71	332,999.54	0.00	7669.85
Culture	Aesthetic landscape	3834.93	54,967.29	37,710.12	211,560.17	0.00	3195.77

to the ecosystem biomass correction factor proposed by Xie et al. (2005) for each province in the study area and selected the average value of 1.42 to calculate each ESV coefficient for different land use types (Table 3).

ESV under scale effects

Based on the exploration of ESV coupling at multiple scales, ESV over different scales can be better analyzed from a spatial perspective. This paper conducted a multi-spatial scale ESV relationship study based on municipal administrative units, county administrative units, and 7.5-km grid cells and used multi-scale cold hotspot spatial clustering to describe the ESV spatial distribution.

ESV sensitivity analysis

Ecological sensitivity (CS) is an important indicator of the degree of dependence of ESV on the value factor. CS was calculated by adjusting the value equivalents of each category upward and downward by 50%, respectively, as follows:

$$CS = \frac{\left(ESV_j - ESV_i\right)/ESV_i}{\left(VC_{jk} - VC_{ik}\right)/VC_{ik}} \tag{4}$$

where the sensitivity index is denoted by CS. If $CS > 1$, it means that ESV is elastic to VC, and if $CS < 1$, it means that ESV is inelastic to VC. ESV represents the total value of ecosystem services; VC_k is the ESV coefficient of land in category K; and j and i represent the ESV before and after the value coefficient adjustment case, respectively.

PLUS model

The PLUS model is based on raster data. It is a patch-generated land use change simulation model coupled with a new land expansion analysis strategy (LEAS) and a CA model based on multiple types of random patch seeds (CARS). PLUS can describe the factors influencing land use change across categories with higher simulation accuracy. This model uses a random forest algorithm to obtain the development probability of each class by extracting land use expansion in period 2 and then simulates and predicts the future land use based on a CA model with multi-class random patch seeds.

Kappa coefficient and FOM coefficient accuracy verification To determine the accuracy of the simulated land use data, 2020 land use data were simulated based on the 2000 and 2010 base period land use data. Actual and simulated data accuracy was verified using Kappa and FOM (Figure of Merit) coefficients. The FOM index for cell-level agreement

has been widely used to quantify the accuracy of land change models (Pontius Jr and Millones 2011; Pontius et al. 2008). The 2020 Kappa coefficient was 0.68, and the FOM was 0.05. The formulas employed are as follows:

$$Kappa = \frac{\sum_{i=1}^{k} n_{ii} - \sum_{i=1}^{k} n_i + n_{+i}}{n^2 - \sum_{i=1}^{k} n_i + n_{+i}} \tag{5}$$

where n is the total number of validation pixels, n_{ii} is the number of correctly classified pixels in class i, n_i is the total number of classified pixels in class i, n_{+i} is the total number of reference pixels in class i, and k is the number of classes.

$$Fom = \frac{B}{A + B + C + D} \tag{6}$$

where A represents the error area caused by actual land use change and is predicted to be unchanged, B represents the area that was accurately predicted, C represents the error area caused by prediction of the wrong land use type, and D represents the error area when no change occurred but it was predicted.

Different scenario settings Based on the Markov module in the PLUS model, four different scenarios of land use types in the HRB in 2030 were constructed. More in detail, the inertia development scenario was based on current land use data for 2020 and predicted the area and spatial distribution of each land use type in 2030. Considering the further promotion of policies related to urban development and county construction in the HRB, the urban development scenario was set to increase the probability of transferring cultivated land, forest, and grassland to construction land by 20% and reduce the probability of transferring construction land to landscape types other than cultivated land by 30%. Considering the protection of ecological patterns in the HRB, in the ecological protection scenario, the probability of transferring cultivated land and forest to construction land was reduced by 40%, while the probability of transferring unused, water, and grassland to construction land was reduced by 20%, and the probability of transferring construction land to forest was increased by 20%. Considering that the HRB is an important grain base in China, in the cultivated land protection scenario, the probability of transferring forest, grassland, water, and unused land to cultivated land was increased by 20%, while the probability of transferring construction land to cultivated land was increased by 30%, and the probability of transferring cultivated land to other land types was reduced by 40%. Under the different scenarios, water, nature reserves, construction land, and cultivated land were used as constraints to limit their arbitrary conversions.

Land use simulation drivers Referring to previous studies (Sun et al. 2022; Jiang et al. 2021; Aytac 2022), a total of 18
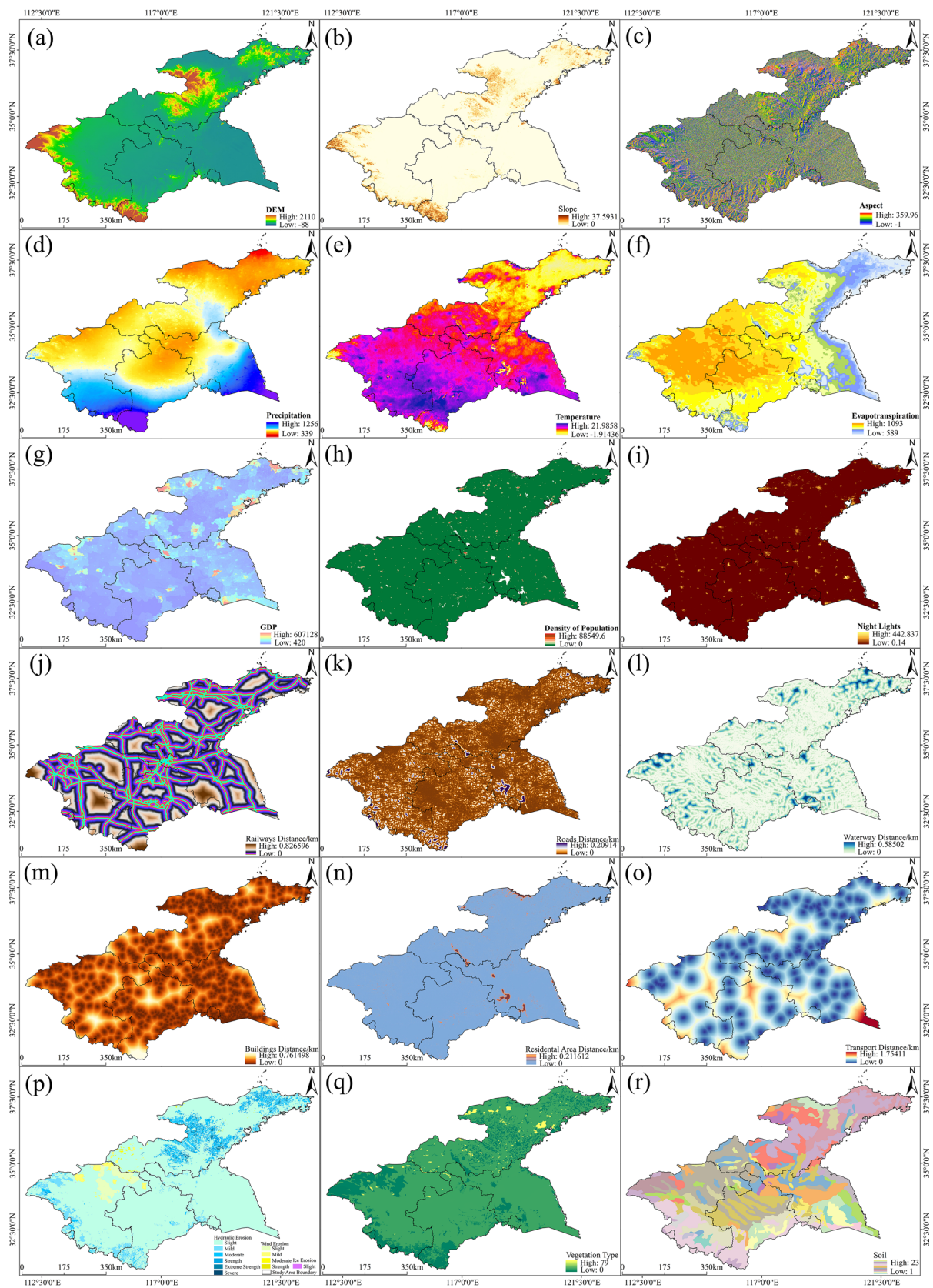
Fig. 3 Drivers of land use evolution

drivers were selected in the PLUS module to simulate land use type changes in five dimensions: topographic, climatic, social, accessibility, and natural (Fig. 3).

ESV hotspot analysis

Hot spot analysis (Getis-Ord G_i^*; Getis and Ord 1992) is commonly used to identify the spatial distribution of cold and hot spot areas. In this paper, hot spot analysis reflected whether ESVs in the HRB had high-value clustering (hot spot) or low-value clustering (cold spot), to determine where clusters occurred in space. The statistical significance of G_i^* was tested using standardized Z values, where a positive and higher Z value indicated tighter clustering for high values (hot spots) and a negative and lower Z value indicated tighter clustering for low values (cold spots).

$$G_i^* = \frac{\sum_{j=1}^{n} w_{ij} x_j}{\sum_{j=1}^{n} x_j} \tag{7}$$

$$Z\left(G_i^*\right) = \frac{\sum_{j=1}^{n} w_{ij} x_j - \overline{X} \sum_{j=1}^{n} w_{ij}}{\sqrt{\frac{n \sum_{j=1}^{n} w_{ij}^2 - \left(\sum_{j=1}^{n} w_{ij}\right)^2}{(n-1)}}} \tag{8}$$

$$S = \sqrt{\frac{1}{n-1} \sum_{j=1}^{n} x_j^2 - \left(\overline{X}\right)^2} \tag{9}$$

where G_i^* is the aggregation index for patch i. w_{ij} is the spatial weight between raster i and j; if the distance between raster i and raster j is within the specified range, $w_{ij} = 1$, otherwise $w_{ij} = 0$. n is the total number of patches; $\overline{X}$ is the mean value of all plaques in the space; and S is the standard deviation of all patch attribute values. The clustering characteristics of the low-value (cold spots) and high-value (hot spots) areas were determined by the Z-values. The ESV cold- and hot-spot partitioning was carried out with reference to previous studies (Zhao et al. 2022; Table 4).

The contribution of land use conversion to ESV

In this paper, the effect of land use change on ESV was analyzed following Zhang et al. (2020), and the contribution of land use conversion to ESV change was calculated as follows:

$$ESCI_{ij} = \frac{\Delta Q_{ij}}{\Delta S_{ij}} \times P_{ij} \tag{10}$$

where $ESCI_{ij}$ is the contribution of land use conversion to ESV change, ΔQ_{ij} quantifies the amount of ESV change from the conversion of land use i to land use j, ΔS_{ij} is the area of land use i converted to land use j, and P_{ij} is the proportion of the area of land use i converted to land use j in the total converted area. When $ESCI > 0$, the contribution is positive and increases as $ESCI$ increases.

Results

Analysis of land use time series change

From 2000 to 2020, the main land use types in the HRB were cultivated land, construction land, and forest (Fig. 4). Cultivated land was the most dominant land type, accounting for 77.80% of the total study area, followed by construction land, accounting for 11.56%, and forest, accounting for 6.35%. Each land type in the district was relatively concentrated; cultivated land was distributed across all directions, while construction land was mainly concentrated in the central and northern parts. Forest was concentrated in the southwest and grassland in the north and west. Except for large lakes where water was concentrated, other water bodies were scattered in patches. Unused land was concentrated in the northern fringe area. Changes in land use type area mainly showed a continuous decrease in cultivated land, grassland, and unused land, a continuous increase in construction land and forest, and an increase followed by a decrease in water. The cultivated land area decreased by 28,344.69 km^2, the grassland area decreased by 2087.81 km^2, the unused land area decreased by 581.88 km^2, the water body area increased by 1511.875 km^2, and the construction land area increased by 26,914.56 km^2. From 2000 to 2010, the cultivated land area changed significantly, decreasing by 15,139.94 km^2.

Table 4 ESV cold and hot spot partitioning

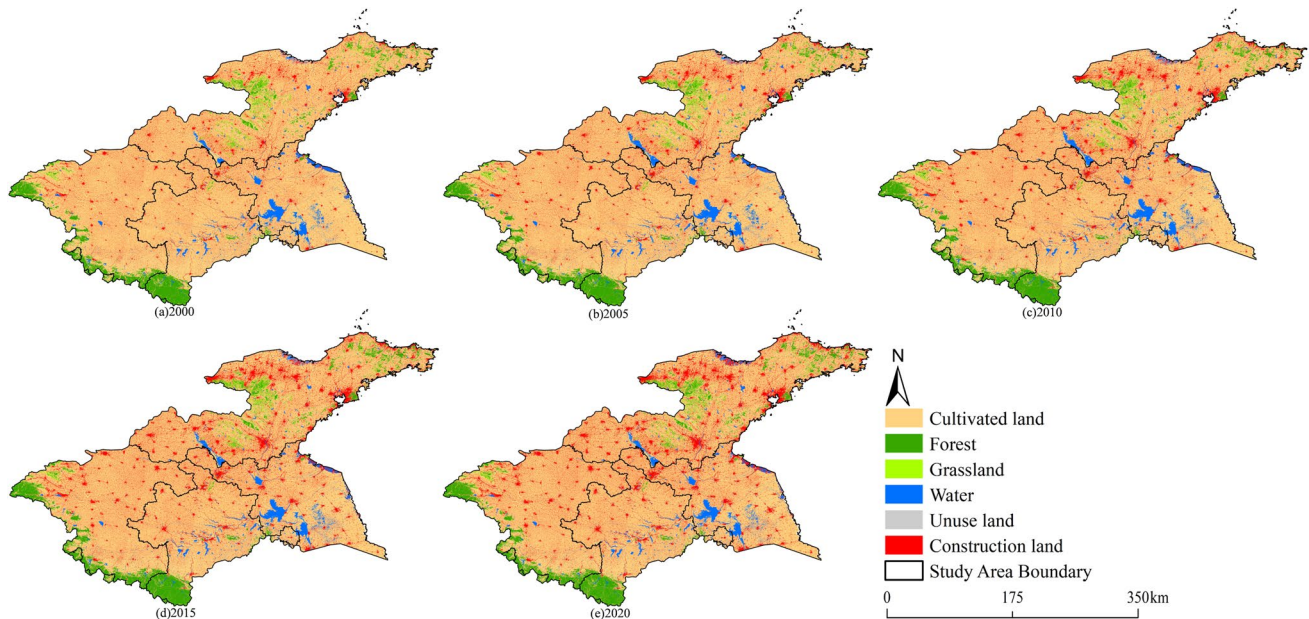| $Z\left(G_i^*\right)$ Value range	≥ 1.35	[0.9, 1.35)	[0.55, 0.9)	(−0.55, 0.55)	(−0.90, −0.55]	(−1.35, −0.90]	≤ -1.35
Zoning type	1	2	3	4	5	6	7
	Highly significant hot spot	Significant hot spot	Hot spot	No significant area	Cold spot	Significant cold spot	Highly significant cold spot

Fig. 4 Land use in the study area from 2000 to 2020

Table 5 Area of land use types (unit: km²)

Year	Cultivated land	Forest	Grassland	Water	Unused land	Construction land
2000	378,337.13	30,861.56	5299.13	14,847.38	754.94	56,193.00
2005	370,592.06	31,619.94	4667.13	17,414.81	661.00	61,338.19
2010	363,197.19	32,193.63	4317.44	17,572.81	534.69	68,477.38
2015	353,434.69	33,727.63	4229.31	16,907.38	429.56	77,564.56
2020	349,992.44	33,450.13	3211.31	16,359.25	173.06	83,107.56

The most significant change in construction land area was an increase of 14,630.19 km² from 2010 to 2020 (Table 5).

Multi-scale ESV estimation and variability analysis

Land use change can cause regional ESV changes. The ESV in the HRB was $222,019 \times 10^{12}$ CNY in 2000, $235,015 \times 10^{12}$ CNY in 2005, $234,419 \times 10^{12}$ CNY in 2010, $229,885 \times 10^{12}$ CNY in 2015, and $224,759 \times 10^{12}$ CNY in 2020, following an overall pattern of a first increase, followed by a decrease. Over the 20 years investigated, the largest change in ESV for water was 0.86×10^{16} CNY. Cultivated land contributed the most to ESV, with a decrease of 0.73×10^{16} CNY over 20 years. In parallel, forest ESV increased by 0.31×10^{16} CNY, grassland ESV decreased by 0.16×10^{16} CNY, and the ESV of unused land changed the least, decreasing by 409,098.86 CNY.

The total ESV in the HRB was calculated using the ArcGIS 10.3 spatial statistics tool and was classified into five major categories using the natural breakpoint method: low, lower, medium, medium–high, and high values (Fig. 5).

Municipal scale, high-value ESVs were located mainly in the south and east, and low-value ESVs were distributed the research area around. At the county scale, ESVs were mainly distributed with low and lower values, with less distribution of medium–high and high values. The low and lower values were mainly distributed in the northwest and west, whereas medium–high and high values were mainly distributed in the south, and medium values were distributed in the central and northern parts of the region. At grid scale, low and lower values occupied most of the area. The median zone was mainly located in the south. Medium–high and high-value grids were clustered and distributed in strips in the middle of the region.

The distribution of land use ESV granularity data classes was not consistent across years at different scales (Fig. 6). Municipal scales were largely unchanged except for 2015, when low-value areas dominated. At the county scale, the distribution was more regular across the years, with mainly low-value areas, followed by lower values. At the grid scale, the variability was higher in 2010 and 2020, lower values dominating in 2010 and 2020.
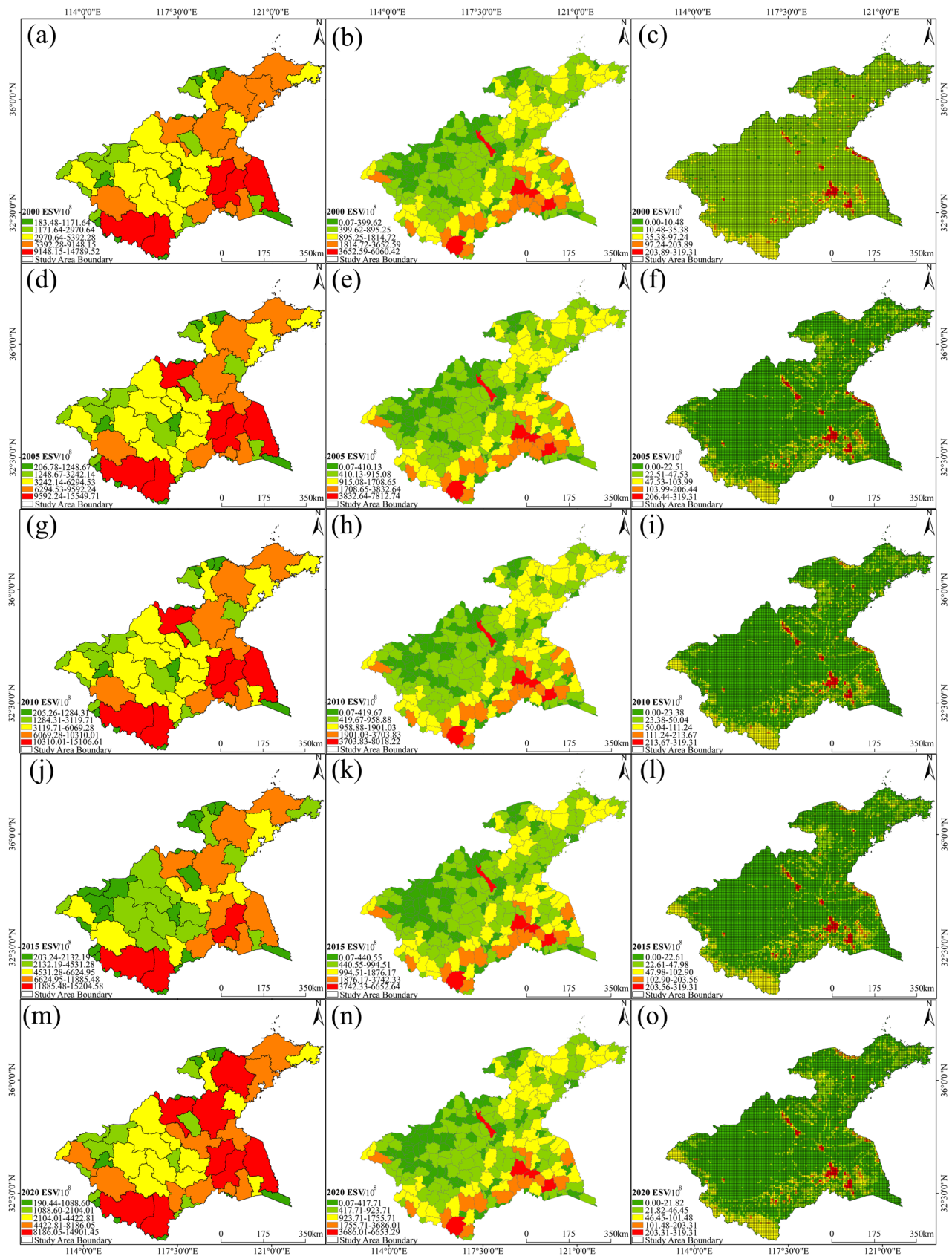
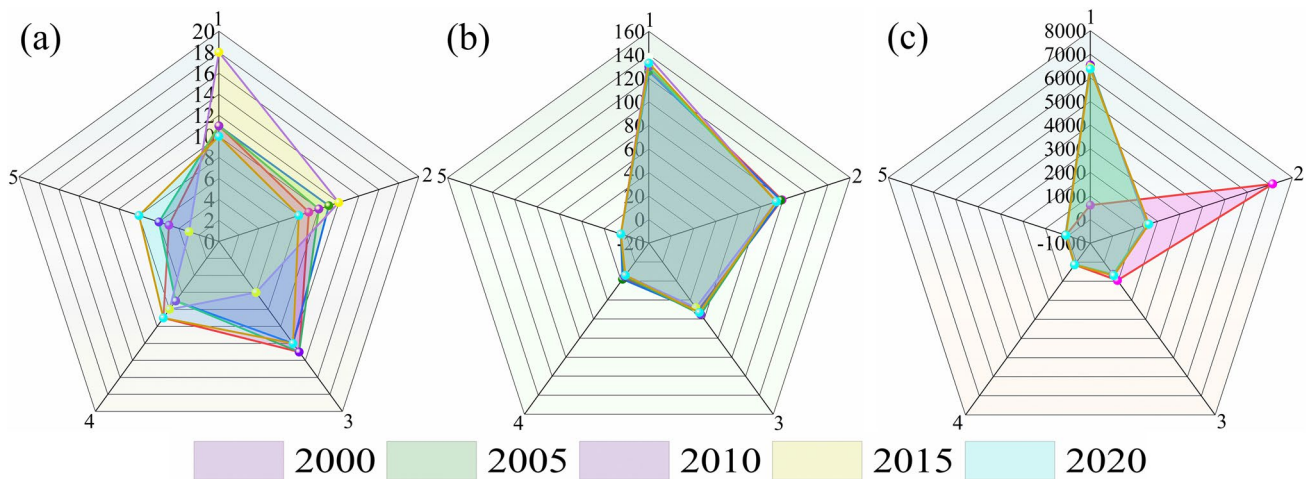**Fig. 5** ESV at multiple scales in the HRB, 2000–2020

Fig. 6 Number of multi-scale ESV particle sizes in the HRB in 2000–2020: **a** municipal scale; **b** county scale; **c** grid scale

Hot spot analysis of ESVs under land use change

The G_i^* hotspot analysis tool was used to explore the spatial clustering characteristics of ESVs at different scales by mapping ESV cold hotspots for the five periods from 2000 to 2020 at three scales: municipal, county, and grid (Fig. 7). ESV spatial distribution characteristics remained unchanged at the same scale, and there were significant differences in the spatial distribution at different scales. At the municipal scale, very significant cold spots and significant cold spots were clustered in the western and northern fringe areas, and cold spots were mainly clustered in the central part. Hot spots, significant hot spots, and very significant hot spots were mainly clustered in the eastern and northeastern edges and parts of the southern region, while the non-significant areas were more dispersed. The cold hot spots had a similar spatial distribution at the county and municipal scales; however, there was high variability at the grid scale. Very significant cold spots were found in scattered patches; significant cold spots and cold spots were concentrated in the northwestern and central regions; non-significant regions were more scattered in distribution; and very significant hot spots were mainly located in the eastern, western, and northwestern fringes and central part of the region, with more significant distribution characteristics.

As can be seen in Fig. 8, the largest percentage of non-significant granularity was found at the municipal and county scales. The cold spot particle size was followed by the significant cold spot particle size at the municipal and county scales. At the grid scale, the significant cold spot particle size was predominant, followed by the non-significant particle size.

Land use change and ESV analysis under multiple scenarios

Multi-scenario land use prediction simulation

Using 2020 as the base period, the land use and expansion changes in the study area in 2010 and 2020 were simulated for 2030 in the HRB under four scenarios by setting different constraints (Fig. 9). The statistics showed a decrease of 12,763 km² in cultivated land under the inertial development scenario compared to the year 2020. Forest area decreased by 301.188 km², grassland area decreased by 619.063 km², water area decreased by 121.188 km², and the areas of unused land and construction land increased by 164.625 km² and 13,639.188 km², respectively. Under the ecological development scenario, forest and construction land areas increased by 652.813 km² and 7,792 km², respectively. Under the cultivated land development scenario, cultivated land area increased significantly by 20,206.563 km². Under the urban development scenario, there was a significant increase in the area of land for construction of 16,634.375 km².

The spatial distribution (Fig. 9) under inertial development (Fig. 9a) exhibited a sharp expansion of construction land, spreading around in a star-like pattern and encroaching on most cultivated land. The central and northern parts received significantly more land for construction, while the southern part had a large area of forest, which was less affected by construction land. Under the cultivated land development scenario (Fig. 9b), there was a dramatic expansion in the area of cultivated land, a large reduction in construction land and forest, and a significant reduction in the area of forest in the south. Under the urban development scenario (Fig. 9c), there was a corresponding encroachment
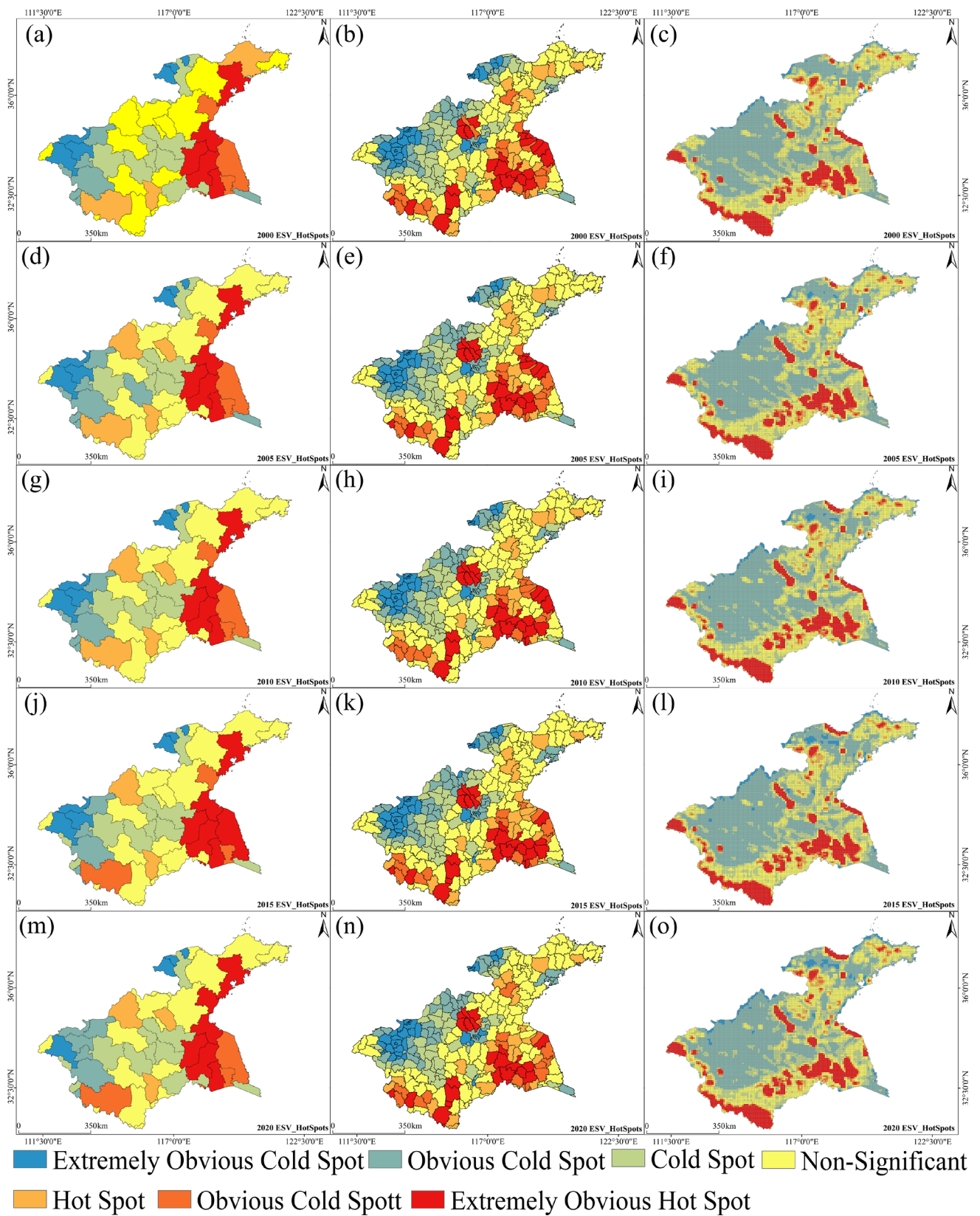
Fig. 7 Multi-scale ESV cold hotspots in the HRB, 2000–2020

Legend:
- Extremely Obvious Cold Spot
- Obvious Cold Spot
- Cold Spot
- Non-Significant
- Hot Spot
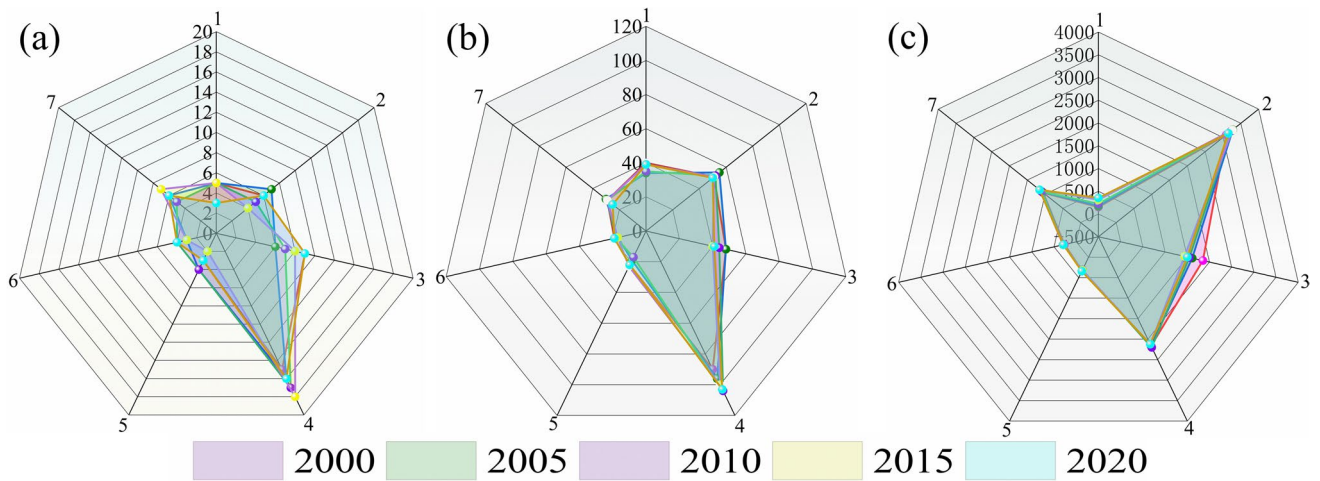- Obvious Cold Spott
- Extremely Obvious Hot Spot

Fig. 8 Number of multi-scale ESV cold and hot spot granularity in the HRB, 2000–2020: **a** municipal scale; **b** county scale; **c** grid scale
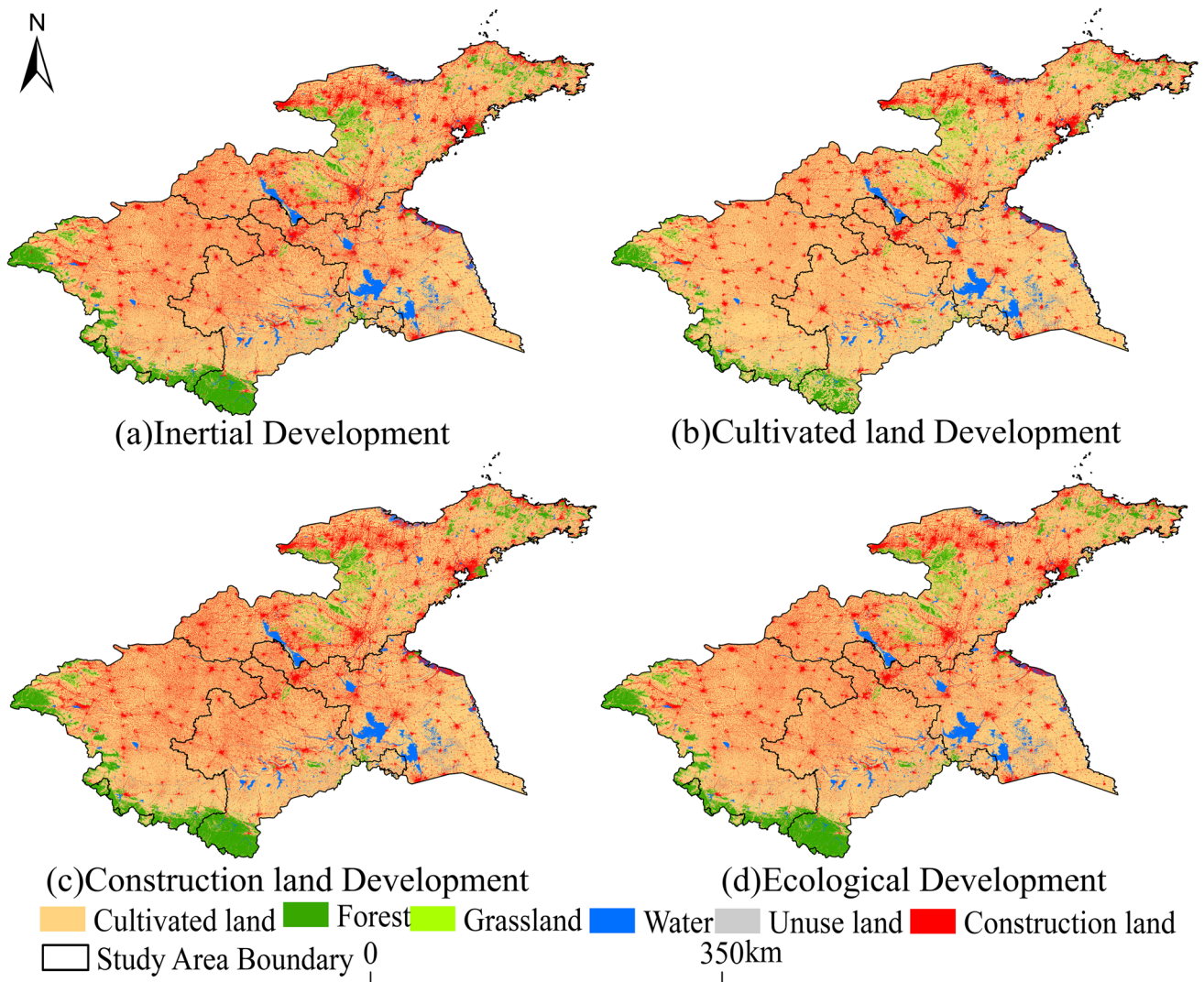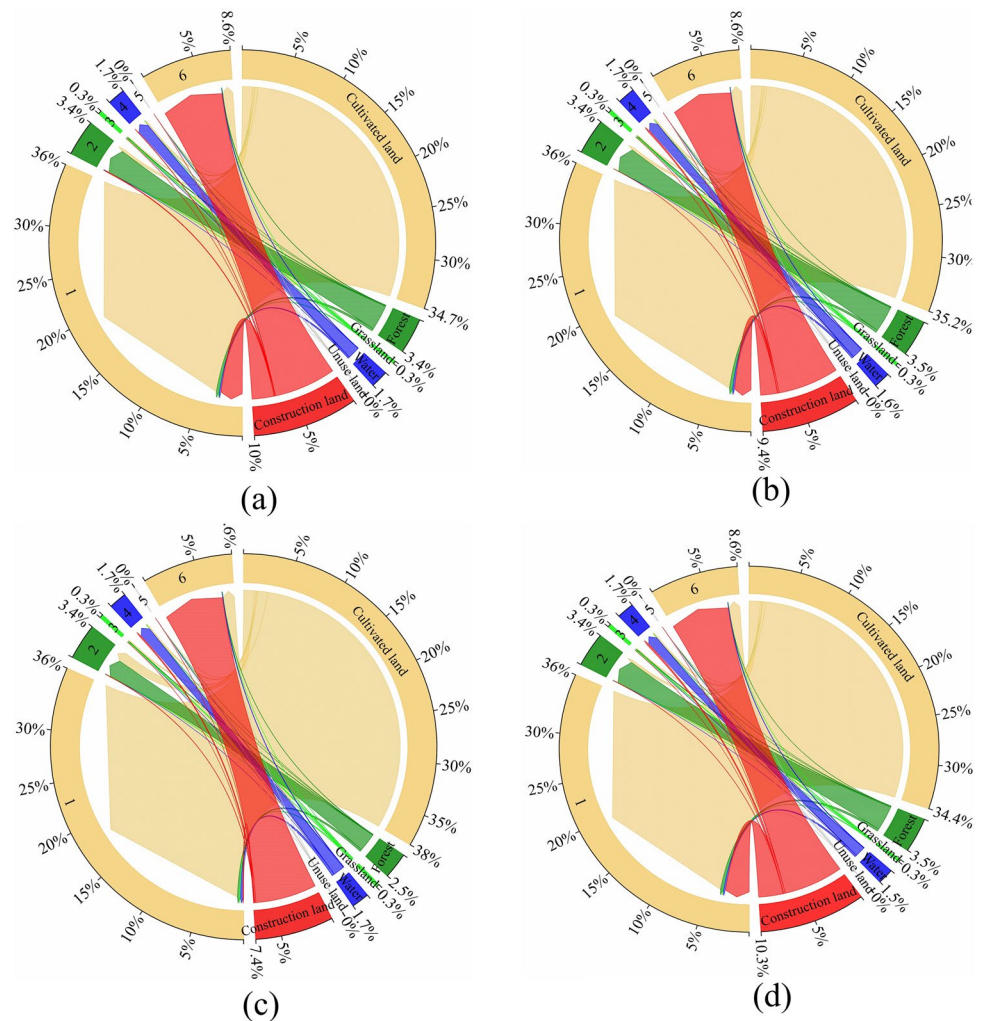

Fig. 9 Simulation of multi-scenario land use projections for 2030

Fig. 10 Multi-scenario land use shifts 2020–2030: **a** inertia; **b** cultivated land; **c** construction land; **d** ecology

of cultivated land area within the expansion of construction land, and complementary area changes between forest, grassland, water, and unused land. Under the ecological development scenario (Fig. 9d), forest area expanded but was still small compared to the total study area, making forestry construction relatively severe.

In relation to land use shifts under multiple scenarios for 2020–2030 (Fig. 10), under inertia development, the total area transferred was 50,430 km², mainly from cultivated land to construction land. Some forest and water areas were transferred out to building sites, resulting in a reduction of water and forest. Under the ecological development scenario, the total transferred area was 46,584.13 km², of which 52.82% of the cultivated land was transferred out and 43.92% of the construction land was transferred in. Cultivated land was developed with a total transferred area of 37,682.56 km², and 70.46% of cultivated land transferred in. Under the urban development scenario, the total transferred area was 56,352.06 km², including 58.93% of cultivated land and 24.16% of construction land that was transferred out, and other land types that shifted to a small extent.

Simulated ESV variability at multiple scales

The ESV of the HRB in 2020 was $224,759 \times 10^{12}$ CNY. ESV declined under all four scenarios, mainly due to construction land expansion (Fig. 11). ESVs under the inertial development, ecological development, cultivated land development, and urban development scenarios were $219,977 \times 10^{12}$ CNY, $218,098 \times 10^{12}$ CNY, $219,757 \times 10^{12}$ CNY, and $213,985 \times 10^{12}$ CNY, respectively. Compared to 2020, in 2030 the inertial development scenario ESV declined by $4,782 \times 10^{12}$ CNY, the ecological development scenario declined by $6,661 \times 10^{12}$ CNY, the cultivated land development scenario declined by $5,002 \times 10^{12}$ CNY, and the urban development scenario declined by $10,774 \times 10^{12}$ CNY. The highest ESV for water was found under the inertial development scenario, at 9.29×10^{16} CNY. The inertial development scenario ESV in 2030 saw a decrease of 687.94×10^{12} CNY compared to 2020 and the highest decrease of cultivated land, $3,271.17 \times 10^{12}$ CNY, under different scenarios, compared to each category of ESV.
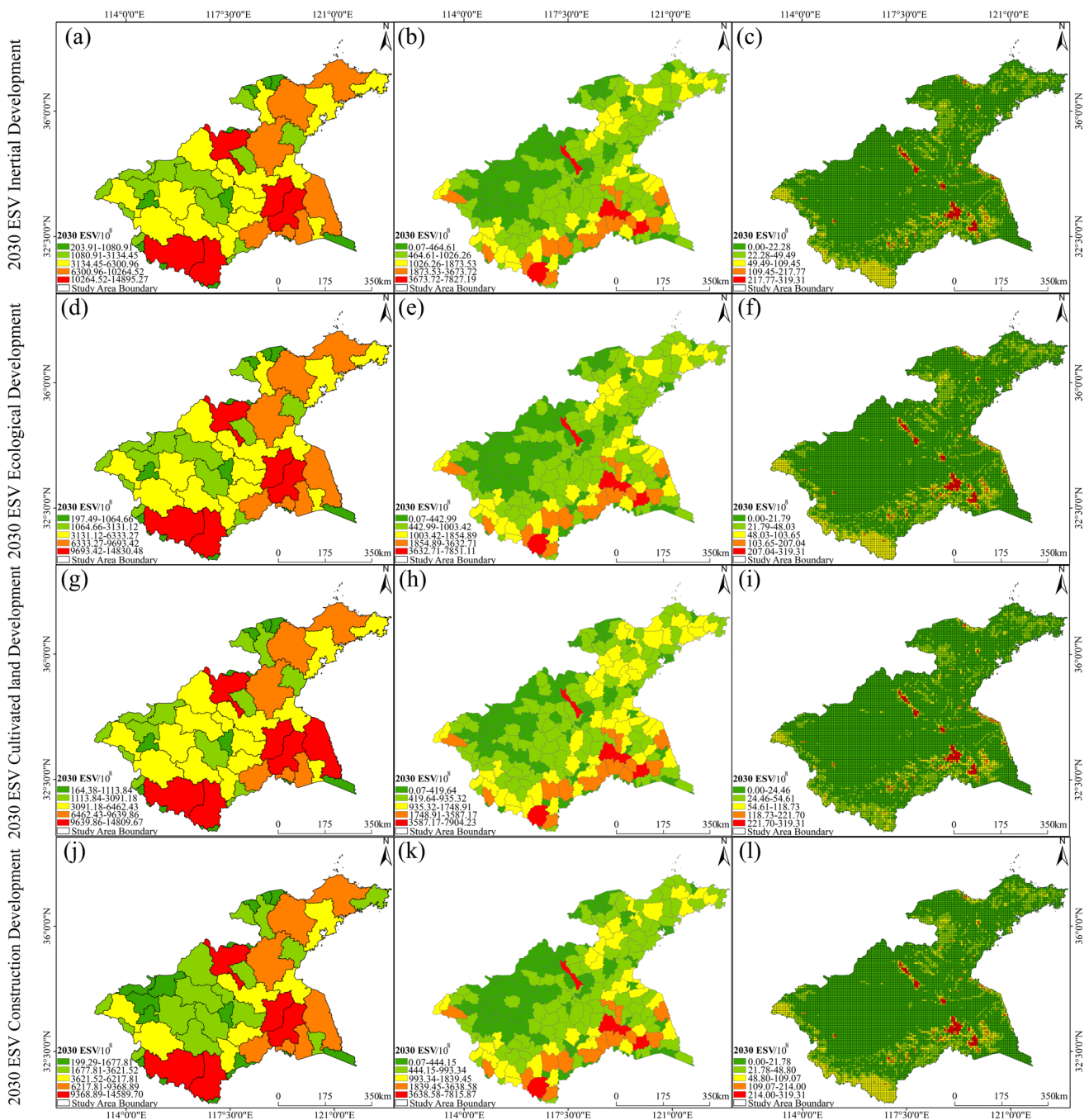
Fig. 11 Multi-scale ESV in the HRB under different scenarios

Under the four scenarios, the highest ESV was 2.927×10^{13} CNY under the ecological development scenario, the highest ESV was 8.79×10^{16} CNY under the cultivated land scenario, and the largest decrease in ESV was 10.774×10^{12} CNY under the urban development scenario.

Changes in the spatial granularity of land use data under different scenarios and scales altered the number of ESV classes (Fig. 12). There was particle size variability when comparing the municipal, county, and grid scale

ESV particle sizes. County and grid scale ESV particle size variability was similar, with low and medium-value areas dominating. At the municipal scale, the median value area was dominant under the inertial development, ecological development, and cultivated land development scenarios, and the low and lower value areas were dominant under the urban development scenario, with small fluctuations in the median, medium–high, and high ESV granularity.
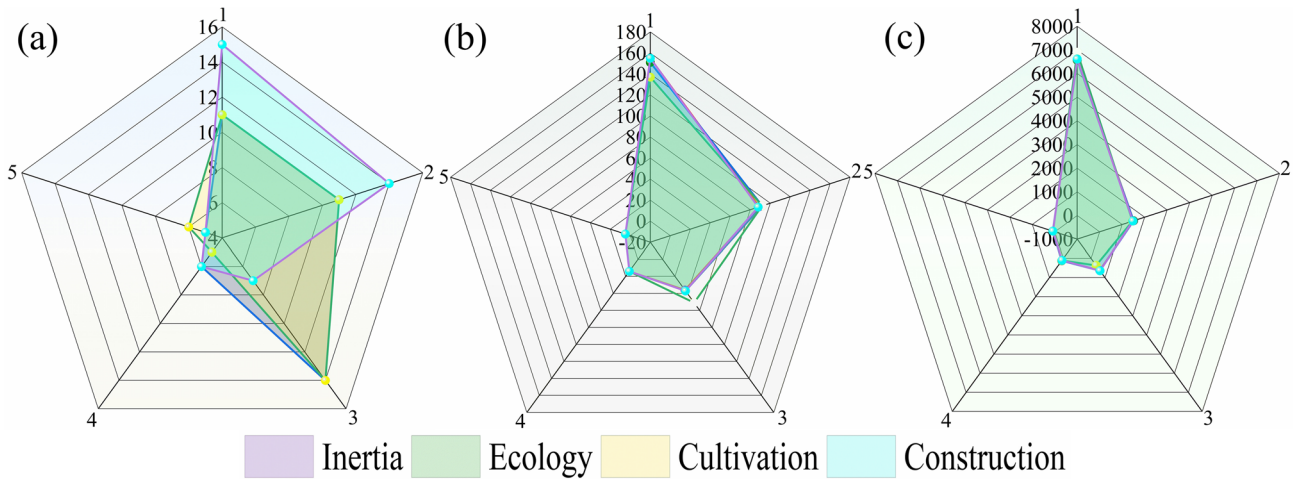
Fig. 12 Number of multi-scale ESV particle sizes under different scenarios in 2030: **a** municipal scale; **b** county scale; **c** grid scale

Cold and hot spot analysis of ESV under multiple scenarios and scales

Based on the ESVs under four different development scenarios in 2030, the spatial distribution of ESV cold and hot spots at different scales was determined using the G_i^* hot spot analysis tool (Fig. 13). Spatially, ESV cold and hot spots were similar at the same scale, with cold spots mainly distributed in the west and central part and hot spots mainly distributed in the east and northeast. There was greater variability at different scales. At the municipal scale, highly significant cold spots, significant cold spots, and cold spots were mainly distributed in the southwest direction. Significant hot spots and highly significant hot spots were mainly distributed in the southeast direction, and non-significant spots were distributed in the north and south directions. At the county scale, highly significant cold spots, significant cold spots, and cold spots were mainly clustered in the west. Hot spots, significant hot spots, and highly significant hot spots were mainly concentrated in the east and south. A small area of highly significant cold spots and hot spots was clustered in the center. At the grid scale, the zone was dominated by significant cold spots and by non-significant and highly significant hot spots. The highly significant cold spots were scattered in a grid distributed in the northwestern fringe, and the highly significant hot spots were mainly distributed in the southwest, south, and east, except for a strip in the center.

The distribution of the number of hot and cold spots at the municipal and county scales was relatively similar in rank. There were mainly non-significant cold and hot spots, whereas the grid scale was dominated by significant cold spots (Fig. 14). Cold and hot spots under the cultivated land development scenario were not consistent in

their spatial clustering characteristics with those in the other three development scenarios. In fact, the non-significant data distribution for cultivated land in the former scenario was lower than that of the other three scenarios at the municipal scale, although there were significantly more hot spots. The number of significant and non-significant cold spots in both the cultivated land development scenarios was lower than in the other three development scenarios at the county scale. At the grid scale, the four development scenarios were mainly clustered around significant cold points, and the highly significant cold points were the least diffused. The cultivated land development scenario had a relatively small percentage of significant cold points and a relatively large percentage of non-significant points, compared to the other three development scenarios.

ESV sensitivity analysis

The sensitivity index values of the value coefficients of land use types in the Huaihe River basin for each year from 2000 to 2030 ranged from 0 to 0.5 (Table 6). In various years, several values of the ESVs sensitivity index CS were lower than 1 for different land types, with low variation inside a same year. This indicated that the ESV in the study area was somewhat inelastic relative to VC and relatively stable. Overall, the land use types in the study area were ranked from highest to lowest in terms of sensitivity index as follows: cultivated land > water > grassland > forest > unused land. The highest sensitivity index value among these land types was 0.4368 for cultivated land in 2000, indicating a 1% reduction in the overall ecological value coefficient, along with a 0.4368% reduction in the ESVs. This was followed by water and forest, due to
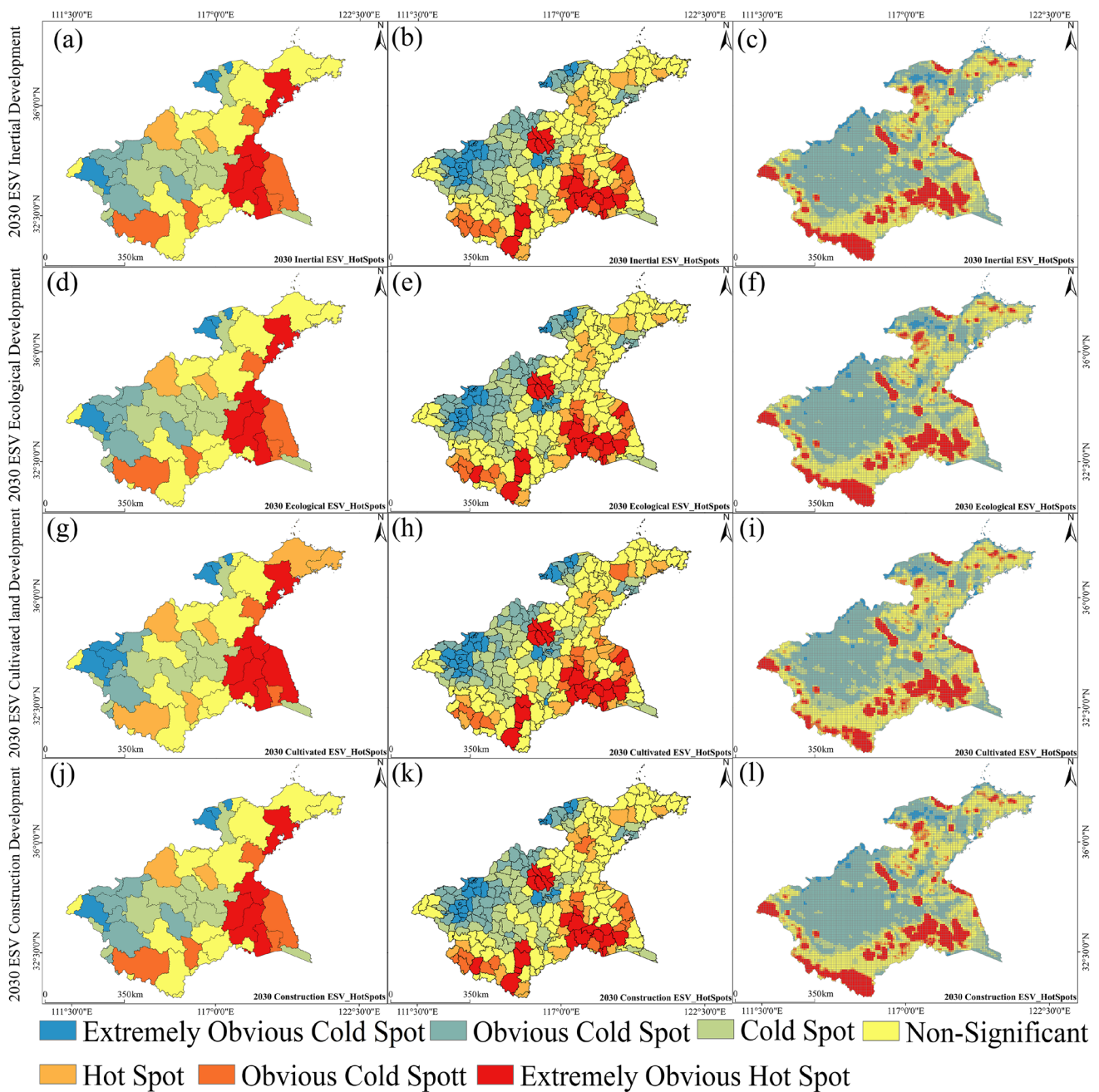
Fig. 13 Distribution of ESV multi-scale cold and hot spots under different scenarios in 2030

the relatively large VC of ecosystem service coefficients of these two land types. After 2015, the lowest value of the sensitivity index of 0.0001 was observed for unused land; this was because the area of this category was small and the service value per unit area was low, and therefore it did not have a significant impact on the total value of the study area. Therefore, the selected coefficients VC of ecosystem service values had little effect on the total ESVs of ESs in the HRB, and the results of the study were fully credible.

Analysis of the contribution of land use conversion to ESV

Land use change had different effects on the ESV across different years (Fig. 15). In the period 2000–2010, the conversion of cultivated land to water had a significant positive impact on ESV, while from 2010 to 2020, the largest positive impact on ESV was observed from the conversion of water to cultivated land. The most significant positive impact on ESV from the transfer of cultivated land and water to each
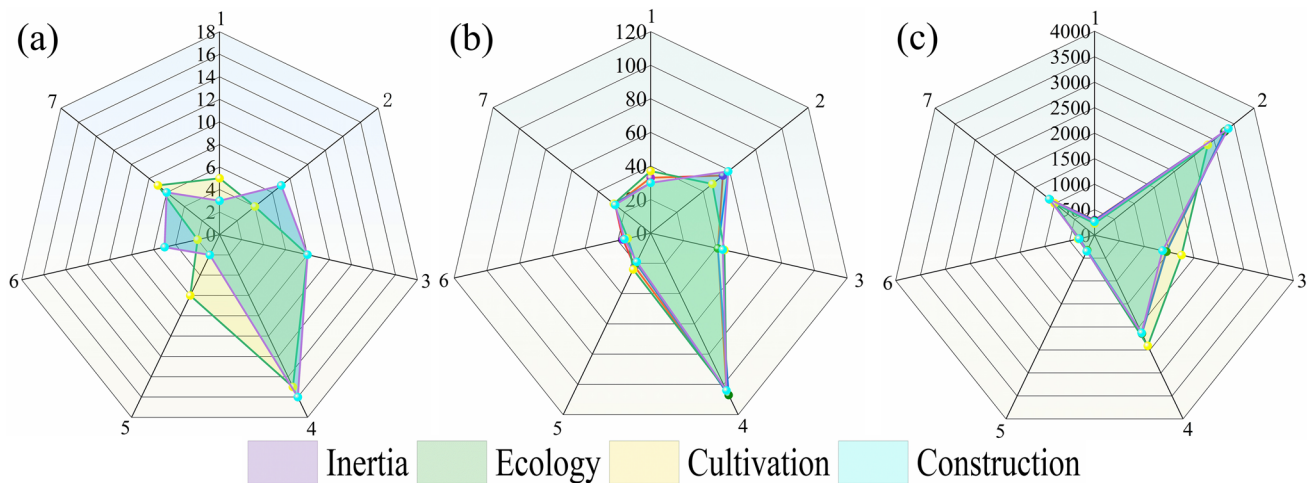
Fig. 14 Number of ESV multi-scale granularity for different scenarios in 2030: **a** municipal scale; **b** county scale; **c** grid scale

Table 6 ESV sensitivity factors for the period 2000–2030

Land use type	2000	2005	2010	2015	2020	Inertial development	Ecological development	Cultivated land development	Construction land development
Cultivated land	0.4368	0.4042	0.3971	0.3940	0.3991	0.3929	0.4029	0.4318	0.4178
Forest	0.1650	0.1597	0.1630	0.1741	0.1766	0.1789	0.1856	0.1307	0.1832
Grassland	0.0184	0.0153	0.0142	0.0142	0.0110	0.0091	0.0092	0.0108	0.0090
Water	0.3796	0.4206	0.4255	0.4175	0.4132	0.4190	0.4022	0.4266	0.3898
Unused land	0.0002	0.0002	0.0002	0.0001	0.0001	0.0001	0.0001	0.0001	0.0001

other was in the 2020–2030 inertial development scenario. The conversion of all land types to unused land had a small impact on ESV, and construction land had a large positive impact on ESV for both cultivated land and forest.

Discussion

Impact of land use change on ESV

The HRB is an important grain and energy base in China, and the conflict between environmental protection and economic development has always been prominent. This study analyzed five periods of historical land use data from 2000 to 2020, simulated future land use development changes under four development scenarios to 2030, assessed the land use changes and ESV in the HRB, and analyzed the spatial distribution of ESV at different scales. The results of this study provide a basis for future land use structure optimization and sustainable development goals. In the past, coal and thermal power resources in the HRB have been used to meet the energy needs of the Chinese government, entailing a serious disturbance of land use and vegetation destruction. However, modern coal production in China has now shifted

from the middle and eastern regions to the west (Wang et al. 2022), and the intensity of coal mining has weakened (Hao et al. 2019). With the rapid development of urbanization and industrialization, construction land continues to encroach on other land. ESV first increased, and then decreased from 2000 to 2020, mainly due to the huge increase in ESV from water and forests, especially coal mining subsidence that created large areas of sunken water (He et al. 2020; Yang et al. 2021), which offset the decrease in ESV due to the loss of cultivated land and other land types. The loss of ESV under multiple scenarios for 2020–2030 was mainly caused by the expansion of construction land (Maimaiti et al. 2022), especially under the cultivated land development scenario where, although the area of cultivated land, water, and construction land increased, this was not sufficient to offset the decrease in ESV due to the decrease in forest area.

Overall ESV trends were aggregated at different scales. ESVs were localized between the same years at the municipal-county-grid scale, and especially at the grid scale, where a grid of low-value areas occupied large areas. This was mainly due to the large area of cultivated land, although the ESV generated by cultivated land was low. This was consistent with the conclusion that cultivated land had a negative effect on ESV (Arowolo A O.et al. 2018). In particular, the fragmentation of

Fig. 15 Contribution of land use change to ESV (2000–2030)

cultivated land caused by large-scale and high-intensity cultivated land development (Yu et al. 2017) caused a decrease in soil fertility and the degradation of large areas of cultivated land, which reduced crop yields and decreased cultivated land ESV. In the cultivated land development scenario, the relative increase in cultivated land area under cultivated land policy protection led to a large reduction in forest, which reduced overall ESV. This was consistent with the results of Fenta et al. (2020), who found that cultivated land-forest conversion led to a decrease in forest ESV.

The overall spatial clustering of ESVs at different scales in a same year became increasingly focused from the municipal to the county and grid scale and top-down. Highly significant hotspots gradually expanded and radiated from the edges toward the interior, with a significant trend from the southeast toward the center. At smaller scales, the regional problem was more focused (Chen et al. 2022), which has important implications

for regional conservation and restoration. Under the 2030 cultivated land development scenario at the county scale, there was lower aggregation of highly significant cold spots, while at the grid scale, there was more aggregation of highly significant cold spots. The impact of human activities on ESV was mainly reflected at the county and grid levels (Zhang et al. 2020); therefore, the systematic explanation of spatial heterogeneity at the grid and regional scales needs to be further explored (Pan et al. 2020). By introducing the degree of contribution of land use conversion to ESV, the impact of the conversion among categories on ESV was further explored, with the conversion of cultivated land to water contributing the most to ESV in 2000–2010, 2000–2020, and 2020–2030 under the ecological development scenarios and in 2020–2030 under the urban development scenario. The highest contribution of the transfer of water to cultivated land was in 2010–2020. In the inertial development scenario for 2020–2030, the highest impact on

ESV was observed from the conversion of cultivated land to water and vice versa, while in the 2020–2030 cultivated land development scenario, the highest impact was from the conversion of cultivated land to water and the second highest from the conversion of water to cultivated land. This was related to the size of the area and of the unit ESV values transferred from cultivated land and water; moreover, the conversion between cultivated land and water indicated increasing disturbance of land use by human activities (Li et al. 2022). Apart from that, the change in unused land had the least impact on ESV; this depended on the size of the transferred area, the low base area of unused land in the study area, and the relatively low area between the other land types transferred.

Limitations and uncertainties

In this study, ESV was estimated due to the lack of statistical data in some county statistical yearbooks. Only 47 municipalities in the study area were considered without county data; moreover, ESV provided by urban greening and ecological parks was ignored, and the ESV generated by construction land was not evaluated. Limited by the land use classification data, this study only macro-classified land use types into six categories; this needs to be further developed in the future using more refined classification data and needs to be verified by actual survey data. In addition, while the PLUS model is a data-driven forecasting model that makes predictions based on historical data, the actual situation may be influenced by other factors. Lastly, further research on the internal drivers of ESs and other service types within cities is needed in the future.

Management and implications for land use and ecosystems in the HRB

Based on the land use-driven change assessment of ESV, the ecological impacts of different land use types were identified. These provide support to decision-makers to optimize land use structure and achieve the sustainable development goals. The rapid urbanization in the southern region of the study area accelerated the transfer of forest to other land types, leading to a continuous decline in forest ESV. Because the southern region is an ecologically protected area, it is necessary to reasonably delineate the urban development boundary (Cao et al. 2021), limit the disorderly expansion of urban open space, actively build ecological corridors, stabilize the ecosystem structure (Andersson et al. 2019), and strictly observe the ecological protection red line. Although the ESVs for large open water and collapsed water areas formed by coal mining subsidence were the highest in the region, further water expansion prevention and control measures are still needed because natural land use transfer is irreversible.

In addition, farmland ecosystems represented the largest area encroached upon during urbanization; therefore, the red line of 1.8 billion acres of cultivated land protection needs to be strictly observed (Zhou et al. 2021). Development should accommodate increasing ESV under urbanization and socio-economic development goals. By setting up four scenarios for land use simulation and analysis, we optimized land use structure, improved land utilization, and provided important references for future ecological construction and land use expansion in the basin. The selection of corresponding scenarios in combination with the development strategy and actual development needs of the HRB is of great significance to achieve regional ecological-social-economic harmony and stability.

Conclusions

(1) From 2000 to 2020, land use patterns in the HRB were mainly cultivated land, construction land, and forest. Of these, cultivated land, grassland, and unused land continued to decline, while construction land and forest increased, and water first increased and then decreased. Under the multiple scenarios for 2020–2030, except for the cultivated land development scenario, in the other three scenarios, the area of cultivated land significantly decreased, the area of construction land increased, and there was low variability among other land types.

(2) From 2000 to 2020, ESV in the HRB first increased and then decreased. From 2020 to 2030, the four scenarios showed ESV declines, with the lowest ESV under the urban development scenario. ESV at different study scales was spatially variable, with high-value areas concentrated in the eastern and central parts of the region and low-value areas concentrated in the western and northern parts of the region. As the study scale declined, the granularity of low-value areas increased, while that of high-value areas decreased.

(3) From the multi-scenario ESV hotspot analysis for 2000–2030, highly significant hot spots and significant hot spots were mainly distributed in the south, eastern fringe regions, and some central regions. Highly significant cold spots and significant cold spots were mainly distributed in the west, northwest fringe regions, and some central regions. The municipal and county scales were mainly dominated by non-significant types, and the grid was dominated by significant cold spots.

(4) Interconversion between cultivated land and water contributed the most to land use ESV, while the conversion of unused land contributed the least to ESV.

Declarations

Ethics approval Not applicable.

Consent to participate Not applicable.

Consent for publication All authors reviewed and approved the manuscript for publication.

Competing interests The authors declare no competing interests.

References

Ana PG, Ilse RG, Francesc B, Philip KR, Alberte B, Wolfgang C (2018) Impacts of urbanization around Mediterranean cities: changes in ecosystem service supply. Ecol Indic 91:589–606. https://doi.org/10.1016/j.ecolind.2018.03.082

Andersson E, Langemeyer J, Borgström S, Mcphearson T, Haase D, Kronenberg J, Baró F (2019) Enabling green and blue infrastructure to improve contributions to human well-being and equity in urban systems. Bioscience 69(7):566–574. https://doi.org/10.1093/biosci/biz058

Arowolo AO, Deng X, Olatunji OA, Obayelu AE (2018) Assessing changes in the value of ecosystem services in response to land-use/land-cover dynamics in Nigeria. Sci Total Environ 636:597–609. https://doi.org/10.1016/j.scitotenv.2018.04.277

Assefa WW, Eneyew BG, Wondie A (2021) The impacts of land-use and land-cover change on wetland ecosystem service values in peri-urban and urban area of Bahir Dar City, Upper Blue Nile Basin Northwestern Ethiopia. Ecol Process 10(1):1–18. https://doi.org/10.1186/s13717-021-00310-8

Ayele AF, Atsushi T, Nigussie H, Mitsuru T, Hiroshi Y, Katsuyuki S, Jian S (2020). Cropland expansion outweighs the monetary effect of declining natural vegetation on ecosystem services in sub-Saharan Africa. Ecosyst Serv, 45, 101154. https://doi.org/10.1016/j.ecoser.2020.101154

Aytaç E (2022) Modeling future impacts on land cover of rapid expansion of hazelnut orchards: a case study on Samsun, Turkey. Eur J Sustain Dev Res 6(4):em0193. https://doi.org/10.21601/ejosdr/12167

Bing G, Xinqi Z, Meichen F (2016) Scenario analysis of sustainable intensive land use based on SD model. Sustain Cities Soc 29:193–202. https://doi.org/10.1016/j.scs.2016.12.013

Braat LC, De GR (2012) The ecosystem services agenda: bridging the worlds of natural science and economics, conservation and development, and public and private policy. Ecosyst Serv 1(1):4–15. https://doi.org/10.1016/j.ecoser.2012.07.011

Cao Y, Kong L, Zhang L, Ouyang Z (2021) The balance between economic development and ecosystem service value in the process of land urbanization: a case study of China's land urbanization from 2000 to 2015. Land Use Policy 108:105536. https://doi.org/10.1016/j.landusepol.2021.105536

Chen H, Yan W, Li Z, Wende W, Xiao S, Wan S, Li S (2022) Spatial patterns of associations among ecosystem services across different spatial scales in metropolitan areas: a case study of Shanghai, China. Ecol Indic 136:108682. https://doi.org/10.1016/j.ecolind.2022.108682

Costanza R, d'Arge R, De Groot R, Farber S, Grasso M, Hannon B, Van Den Belt M (1997) The value of the world's ecosystem services and natural capital. Nature 387(6630):253–260. https://doi.org/10.1038/387253a0

Crossman ND, Bryan BA (2009) Identifying cost-effective hotspots for restoring natural capital and enhancing landscape multifunctionality. Ecol Econ 68(3):654–668. https://doi.org/10.1016/j.ecolecon.2008.05.003

Crossman ND, Bryan BA, Summers DM (2011) Carbon payments and low-cost conservation. Conserv Biol 25(4):835–845. https://doi.org/10.1111/j.1523-1739.2011.01649.x

Cumming GS, Buerkert A, Hoffmann EM, Schlecht E, von Cramon-Taubadel S, Tscharntke T (2014) Implications of agricultural transitions and urbanization for ecosystem services. Nature 515(7525):50–57. https://doi.org/10.1038/nature13945

Defeng Z, Yanhui W, Shuai H, Wenjing X, Leting L, & Shuai Y (2020). Spatial-temporal variation and tradeoffs/synergies analysis on multiple ecosystem services: a case study in the Three-River Headwaters region of China. Ecol Indic, 116, 106494. https://doi.org/10.1016/j.ecolind.2020.106494

Fan Q, Yang X, Zhang C (2022) A review of ecosystem services research focusing on China against the background of urbanization. Int J Env Res Pub He 19(14):8271. https://doi.org/10.3390/ijerph19148271

Fenta AA, Tsunekawa A, Haregeweyn N, Tsubo M, Yasuda H, Shimizu K, Sun J (2020) Cropland expansion outweighs the monetary effect of declining natural vegetation on ecosystem services in sub-Saharan Africa. Ecosyst Serv 45:101154. https://doi.org/10.1016/j.ecoser.2020.101154

Gao X, Wang J, Li C, Shen W, Song Z, Nie C, Zhang X (2021) Land use change simulation and spatial analysis of ecosystem service value in Shijiazhuang under multi-scenarios. Environ Sci Pollut Res 28(24):31043–31058. https://doi.org/10.1007/s11356-021-12826-9

Gaodi X, Caixia Z, Lin Z, Leiming Z (2017) Dynamic changes in the value of China's ecosystem services. Ecosyst Serv 26:146–154. https://doi.org/10.1016/j.ecoser.2017.06.010

García-Nieto AP, Geijzendorffer IR, Baró F, Roche PK, Bondeau A, Cramer W (2018) Impacts of urbanization around Mediterranean cities: changes in ecosystem service supply. Ecol Indic 91:589–606. https://doi.org/10.1016/j.ecolind.2018.03.082

Gashaw T, Tulu T, Argaw M, Worqlul AW, Tolessa T, Kindu M (2018) Estimating the impacts of land use/land cover changes on ecosystem service values: the case of the Andassa watershed in the upper Blue Nile basin of Ethiopia. Ecosyst Serv 31:219–228. https://doi.org/10.1016/j.ecoser.2018.05.001

Getis A, Ord JK (1992) The analysis of spatial association by use of distance statistics. Geogr Anal 24(3):189–206. https://doi.org/10.1111/j.1538-4632.1992.tb00261.x

Groot DR, Brander L, Ploeg DVS, Constanza R et al (2012) Global estimates of the value of ecosystems and their services in monetary units. Ecosyst Services 1(1):50–61. https://doi.org/10.1016/j.ecoser.2012.07.005

Guzman LA, Escobar F, Peña J, Cardona R (2020) A cellular automata-based land-use model as an integrated spatial decision support system for urban planning in developing cities: the case of the

Bogotá region. Land Use Policy 92:104445. https://doi.org/10.1016/j.landusepol.2019.104445

Hao X, Song M, Feng Y, Zhang W (2019) Decapacity policy effect on China's coal industry. Energies 12(12):2331. https://doi.org/10.3390/en12122331

He T, Xiao W, Zhao Y, Deng X, Hu Z (2020) Identification of water-logging in eastern China induced by mining subsidence: a case study of Google earth engine time-series analysis applied to the Huainan coal field. Remote Sens Environ 242:111742. https://doi.org/10.1016/j.rse.2020.111742

Hu S, Yang Y, Li A, Liu K, Mi C, Shi R (2022). Integrating ecosystem services into assessments of sustainable development goals: a case study of the Beijing-Tianjin-Hebei Region, China. Front Environ Sci, 629. https://doi.org/10.3389/fenvs.2022.897792

Huang R, Nie Y, Duo L, Zhang X, Wu Z, Xiong J (2021) Construction land suitability assessment in rapid urbanizing cities for promoting the implementation of United Nations sustainable development goals: a case study of Nanchang, China. Environ Sci Pollut Res 28:25650–25663. https://doi.org/10.1007/s11356-020-12336-0

Jiang Y, Huang M, Chen X, Wang Z, Xiao L, Xu K, Shi Z (2021). Identification and risk prediction of potentially contaminated sites in the Yangtze River Delta. Sci Total Environ, 815, 151982. https://doi.org/10.1016/j.scitotenv.2021.151982

Jinghu P, Shimei W, Zhen L (2020). Spatiotemporal pattern of trade-offs and synergistic relationships among multiple ecosystem services in an arid inland river basin in NW China. Ecol Indic, 114, 106345. https://doi.org/10.1016/j.ecolind.2020.106345

Li SC (2019) Reflections on ecosystem service research. Landsc Arch Front 7(01):82–87

Lede N, Mei P, Yan Z (2020) Research on dynamic simulation and prediction of urban expansion based on SLEUTH model. Intl J Eng Syst Modell Simul 11(4):222–234. https://doi.org/10.1504/IJESMS.2020.111272

Lede N, Mei P (2021) Research on dynamic simulation of land use change based on geographical weighted CLUE-S model. Intl J Environ Technol Manag 24(1–2):49–61. https://doi.org/10.1504/IJETM.2021.115728

Leon CB, Rudolf DG (2012) The ecosystem services agenda: bridging the worlds of natural science and economics, conservation and development, and public and private policy. Ecosyst Serv 1(1):4–15. https://doi.org/10.1016/j.ecoser.2012.07.011

Li F, Zhang S, Yang J, Bu K, Wang Q, Tang J, Chang L (2016) The effects of population density changes on ecosystem services value: a case study in Western Jilin, China. Ecol Indic 61:328–337. https://doi.org/10.1016/j.ecolind.2015.09.033

Li J, Dong S, Li Y, Wang Y, Li Z, Li F (2022). Effects of land use change on ecosystem services in the China-Mongolia-Russia economic corridor. J Clean Prod, 132175. https://doi.org/10.1016/j.jclepro.2022.132175

Liang X, Guan Q, Clarke KC, Liu S, Wang B, Yao Y (2021). Understanding the drivers of sustainable land expansion using a patch-generating land use simulation (PLUS) model: a case study in Wuhan, China. Computers, Environment and Urban Systems, 85, 101569. https://doi.org/10.1016/j.compenvurbsys.2020.101569

Liu P, Hu Y, & Jia W (2021). Land use optimization research based on FLUS model and ecosystem services-setting Jinan City as an example. Urban Climate, 40, 100984. https://doi.org/10.1016/j.uclim.2021.100984

Maimaiti B, Chen S, Kasimu A, Mamat A, Aierken N, Chen Q (2022) Coupling and coordination relationships between urban expansion and ecosystem service value in Kashgar City. Remote Sens-Basel 14(11):2557. https://doi.org/10.3390/rs14112557

Liu W, Zhan J, Zhao F, Yan H, Zhang F, Wei X (2019) Impacts of urbanization-induced land-use changes on ecosystem services: a case study of the Pearl River Delta metropolitan region, China.

Ecol Indic 98:228–238. https://doi.org/10.1016/j.ecolind.2018.10.054

Niu L, Pan M (2021) Research on dynamic simulation of land use change based on geographical weighted CLUE-S model. Int J Environ Technol Manag 24(1–2):49–61. https://doi.org/10.1504/IJETM.2021.115728

Pan J, Wei S, Li Z (2020) Spatiotemporal pattern of trade-offs and synergistic relationships among multiple ecosystem services in an arid inland river basin in NW China. Ecol Indic 114:106345. https://doi.org/10.1016/j.ecolind.2020.106345

Song W, Deng X (2017) Land-use/land-cover change and ecosystem service provision in China. Sci Total Environ 576:705–719. https://doi.org/10.1016/j.scitotenv.2016.07.078

Pontius RG Jr, Millones M (2011) Death to Kappa: birth of quantity disagreement and allocation disagreement for accuracy assessment. Int J Remote Sens 32(15):4407–4429. https://doi.org/10.1007/s00168-007-0138-2

Pontius RG, Boersma W, Castella J, Clarke K, Nijs T, Dietzel C, Kok K (2008) Comparing the input, output, and validation maps for several models of land change. Ann Reg Sci 42(1):11–37. https://doi.org/10.1007/s00168-007-0138-2

Robert C, Ralph D, Rudolf DG, Stephen F, Monica G, Bruce H, Marjan VDB (1997). The value of the world's ecosystem services and natural capital. Nature: International Weekly Journal of Science, 387(6630), 253–260. https://doi.org/10.1038/387253a0

Temesgen G, Taffa T, Mekuria A, Abeyou WW, Terefe T, Mengistie K (2018) Estimating the impacts of land use/land cover changes on ecosystem service values: the case of the Andassa watershed in the Upper Blue Nile basin of Ethiopia. Ecosyst Serv 31:219–228. https://doi.org/10.1016/j.ecoser.2018.05.001

Tingting H, Wu X, Yanling Z, Xinyu D, Zhenqi H (2020) Identification of waterlogging in Eastern China induced by mining subsidence: a case study of Google Earth Engine time-series analysis applied to the Huainan coal field. Remote Sens Environ 242:111742. https://doi.org/10.1016/j.rse.2020.111742

Sun J, Li G, Zhang Y, Qin W, Wang M (2022) Identification of priority areas for afforestation in the loess plateau region of China. Ecol Indic 140:108998. https://doi.org/10.1016/j.ecolind.2022.108998

Tan Z, Guan Q, Lin J, Yang L, Luo H, Ma Y, Wang N (2020) The response and simulation of ecosystem services value to land use/land cover in an oasis, Northwest China. Ecol Indic 118:106711. https://doi.org/10.1016/j.ecolind.2020.106711

Wang Y, Wang X, Wang H, Zhang X, Zhong Q, Yue Q, Liang S (2022) Human health and ecosystem impacts of China's resource extraction. Sci Total Environ 847:157465. https://doi.org/10.1016/j.scitotenv.2022.157465

Wei S, Xiang ZD (2017) Land-use/land-cover change and ecosystem service provision in China. Sci Total Environ 576:705–719. https://doi.org/10.1016/j.scitotenv.2016.07.078

Xie G, Zhang C, Zhen L, Zhang L (2017) Dynamic changes in the value of China's ecosystem services. Ecosyst Serv 26:146–154. https://doi.org/10.1016/j.ecoser.2017.06.010

Xie GD, Zhang C, Zhang L, Chen W, Li S (2015) Improvement of the evaluation method for ecosystem service value based on per unit area. J Natl Resour 30(08):1243–1254

Xie GD, Zhen L, Lu CX, Xiao Y, Chen C (2008) Expert knowledge based valuation method of ecosystem services in China. J Natl Resour 05:911–919

Xie GD, Xiao Y, Zhen L, Lu CX (2005) Study on ecosystem services value of food production in China. Chinese J Eco-Agri 03:10–13

Xie L, Wang H, Liu S (2022) The ecosystem service values simulation and driving force analysis based on land use/land cover: a case study in inland rivers in arid areas of the Aksu River Basin China. Ecol Indic 138:108828. https://doi.org/10.1016/j.ecolind.2022.108828

Xueru Z, Wei S, Yanqing L, Xiaomiao F, Quanzhi Y, Jingtao W (2020) Land use changes in the coastal zone of China's Hebei Province and the corresponding impacts on habitat quality. Land Use Policy 99:104957. https://doi.org/10.1016/j.landusepol.2020.104957

Xu GH, Mei S, Yunan F, Wen Z (2019) De-capacity policy effect on China's coal industry. Energies 12(12):2331. https://doi.org/10.3390/en12122331

Yang Y, Zhang Y, Su X, Hou H, Zhang S (2021) The spatial distribution and expansion of subsided wetlands induced by underground coal mining in eastern China. Environ Earth Sci 80(3):112. https://doi.org/10.1007/s12665-021-09422-y

Ye Y, Zhang J, Wang T, Bai H, Wang X, Zhao W (2021) Changes in land-use and ecosystem service value in Guangdong Province, Southern China, from 1990 to 2018. Land 10(4):426. https://doi.org/10.3390/land10040426

Yu Q, Hu Q, van Vliet J, Verburg PH, Wu W (2017) GlobeLand30 shows little cropland area loss but greater fragmentation in China. Intl J Appl Earth Observ Geoinform 66:37–45. https://doi.org/10.1016/j.jag.2017.11.002

Zhang X, Song W, Lang Y, Feng X, Yuan Q, Wang J (2020) Land use changes in the coastal zone of China's Hebei Province and the corresponding impacts on habitat quality. Land Use Policy 99:104957. https://doi.org/10.1016/j.landusepol.2020.104957

Zhe T, Qing YG, Jinkuo L, Liqin Y, Hai PL, Yun RM, Ning W (2020) The response and simulation of ecosystem services value to land use/land cover in an oasis Northwest China. Ecol Indic 118:106711. https://doi.org/10.1016/j.ecolind.2020.106711

Zhou Y, Li X, Liu Y (2021) Cultivated land protection and rational use in China. Land Use Policy 106:105454. https://doi.org/10.1016/j.landusepol.2021.105454

Zhao XQ, Shi XQ, Li YH, Li YM, Huang P (2022) Spatio-temporal pattern and functional zoning of ecosystem services in the karst mountainous areas of southeastern Yunnan. Acta Geographica Sinica 77(03):736–756. https://doi.org/10.11821/dlxb20220301

Zheng D, Wang Y, Hao S, Xu W, Lv L, Yu S (2020) Spatial-temporal variation and tradeoffs/synergies analysis on multiple ecosystem services: a case study in the Three-River headwaters region of China. Ecol Indic 116:106494. https://doi.org/10.1016/j.ecolind.2020.106494

Authors and Affiliations

Xuyang Zhang[1] · Yuzhi Zhou[1] · Linli Long[1] · Pian Hu[1] · Meiqin Huang[1] · Wen Xie[1] · Yongchun Chen[3] · Xiaoyang Chen[1,2]

Xuyang Zhang
zxy374260025@163.com

Yuzhi Zhou
2021208@aust.edu.cn

Linli Long
long6_6@163.com

Pian Hu
2451747054@qq.com

Meiqin Huang
2900413866@qq.com

Wen Xie
781255491@qq.com

Yongchun Chen
421774469@qq.com

[1] School of Earth and Environment, Anhui University of Science and Technology, Huainan 232001, Anhui, China

[2] Anhui Engineering Laboratory for Comprehensive Utilization of Water and Soil Resources & Ecological Protection in Mining Area With High Groundwater Level, Huainan 232001, Anhui, China

[3] Ping'an Coal Mining Engineering Technology Research Institute Co., Ltd, Huainan 232001, Anhui, China